

Local Harmonic Approximation to Quantum Mean Force Gibbs State

Prem Kumar^{1,2,*}

¹*Optics and Quantum Information Group, The Institute of Mathematical Sciences,
C.I.T. Campus, Taramani, Chennai 600113, India.*

²*Homi Bhabha National Institute, Training School Complex, Anushakti Nagar, Mumbai 400094, India.*

When the strength of interaction between a quantum system and bath is non-negligible, the equilibrium state can deviate from the Gibbs state. Here, we obtain an approximate expression for such a mean force Gibbs state for a particle in an arbitrary one dimensional potential, interacting with a bosonic bath. This approximate state is accurate when either the system-bath coupling or the temperature is large, or when the third and higher derivatives of the potential are small compared to certain system-bath specific parameters. We show that our result recovers the ultra strong coupling and high temperature results recently derived in literature. We then apply this method to study some systems like a quartic oscillator and a particle in a quartic double-well potential. We also use our method to analyze the proton tunneling problem in a DNA recently studied in literature [Slocombe et al., *Comm. Phys.*, vol. 5, no. 1, p. 109, 2022], where our results suggest the equilibrium value of the probability of mutation to be orders of magnitude lower than the steady state value obtained there (10^{-8} vs 10^{-4}).

I. INTRODUCTION

Continuous variable (CV) quantum systems have been immensely studied in the context of fields like quantum information processing, communication and computation [1–7], quantum resource theories and thermodynamics [8–10], quantum technology [11, 12], quantum chaos [13–16] and open quantum system [17–24]. Thermodynamic equilibrium properties of these CV systems are hence of great interest in many of these studies and applications. But when the strength of interaction between a quantum system and bath is non-negligible, the equilibrium state can deviate from the Gibbs state and is given by the mean force Gibbs state (MFGS)[25], defined as,

$$\rho = \text{Tr}_R \left[\frac{e^{-\beta H_{tot}}}{Z} \right] \quad (1)$$

where H_{tot} is the full system-bath Hamiltonian and the partial trace is taken over the bath degrees of freedom. The MFGS has found several applications in fields like strong coupling quantum thermodynamics [26–29] and quantum chemistry [30–33] and is relevant to many other problems in quantum chemistry and biology.

For example, consider a particle in a double well (DW) potential [20–23, 34, 35] interacting with a bosonic bath which finds application, for example, in quantum chemistry and biology to study processes like chemical reactions occurring in the presence of a solvent [36–39]. Finding an analytical expression MFGS for such a system is hence of interest. But most of these physical processes happen in the intermediate coupling regime, where an analytical expression for MFGS is not available. By intermediate coupling regime, we mean the regime in which the bath induced timescales on the system are of the same

order as the timescales associated with the bath itself (e.g., $\hbar/k_B T$) [40].

Analytical expressions for MFGS in weak and ultra strong coupling (USC) limits were derived recently [25]. Further, corrections to the USC regime MFGS have been evaluated using dynamics [41] and perturbative expansion methods [42]. Additionally, high temperature expansion for the MFGS was also derived recently [43, 44].

If the CV system is a harmonic oscillator (HO), then the expression for the MFGS is known analytically [45, 46]. But for a particle in an arbitrary 1D potential $V(q)$, analytical expression for MFGS in intermediate coupling regime remains a challenge. Recently, two numerically exact approaches, “Time Evolving matrix Product Operator” (TEMPO) [47–52] and “The hierarchical equations of motion” (HEOM) [35, 38, 53], have made these MFGS and steady state calculations much more computationally efficient. But for a particle in an arbitrary 1D potential $V(q)$, the system is infinite dimensional and a typical numerical technique proceeds by truncating the system in energy eigenbasis [54]. In the intermediate coupling regime, this is an issue because the effective dimension of the system increases with the coupling, causing the calculation to become computationally very expensive.

Here, we provide an approximate analytical expression for the MFGS, which we call local harmonic approximation (LHA) to MFGS, for a particle in a 1D potential $V(q)$ interacting with a non interacting bosonic bath. This method is accurate when either the system-bath coupling or the temperature is large, or when the third and higher derivatives of the potential are small compared to certain system-bath specific parameters. We find that LHA reduces to the exact USC and high temperature results in the appropriate limits [25, 43].

In [Sec. II](#), we provide our main results. In [Sec. III](#), we use LHA to study some CV open quantum systems, like a quartic oscillator and a quartic double well potential. [Sec. III C](#) provides an application of LHA to the proton

* premkr@imsc.res.in; prem3141592@gmail.com

tunneling problem in DNA that has been recently investigated by Slocombe et al. [36, 37]. **Sec. IV** provides conclusion and discussions.

II. MAIN RESULTS

We consider a particle of mass m in an arbitrary potential $V(q)$, linearly coupled to a bath of harmonic oscillators. This system is described by the Hamiltonian,

$$H = \frac{p^2}{2m} + V(q) + \sum_k \left[\frac{p_k^2}{2m_k} + \frac{1}{2} m_k \omega_k^2 \left(q_k - \frac{c_k q}{m_k \omega_k^2} \right)^2 \right], \quad (2)$$

where ω_k , m_k , and c_k are the frequency, mass, and coupling strength of the k th oscillator, respectively. For simplicity, we assume a one dimensional system, though our results are easily generalized to higher dimensions. Here and throughout, we assume $\hbar = 1$. Throughout this article we write operator matrix elements in position basis as $O(q, \eta) = \langle q + \eta | \hat{O} | q - \eta \rangle$. Diagonal elements are obtained when $\eta = 0$ and will be denoted by $O(q) = O(q, 0)$.

Upon integrating out the bath degrees of freedom, the MFGS for the particle can be expressed as a Euclidean path integral [46],

$$\rho(q, \eta) = Z_R^{-1} \int_{q+\eta}^{q-\eta} \mathcal{D}q(\tau) e^{-S_0[q(\tau)] - \Phi[q(\tau)]} \quad (3)$$

where, $\int_x^y \mathcal{D}q(\tau)$ signifies $q(0) = x$ and $q(\beta) = y$ in the functional integral. The reduced partition function is the ratio of bath and system+bath partition functions, $Z_R = Z/Z_B$, and

$$S_0[q(\tau)] = \int_0^\beta d\tau \left(\frac{1}{2} m \dot{q}(\tau)^2 + V(q(\tau)) \right) \quad (4)$$

$$\Phi[q(t)] = \frac{1}{4} \int_0^\beta d\tau \int_0^\beta d\tau' K(\tau - \tau') (q(\tau) - q(\tau'))^2 \quad (5)$$

are the action for the free particle and the influence action, respectively. The bath correlation function is defined as,

$$K(\tau) = \int_0^\infty d\omega J(\omega) \frac{\cosh[\omega(\beta/2 - \tau)]}{\sinh[\omega\beta/2]} \quad (6)$$

in terms of the spectral density

$$J(\omega) = \alpha \sum_k \frac{c_k^2}{2m_k \omega_k} \delta(\omega - \omega_k), \quad (7)$$

where we have introduced the dimensionless number α to characterize the strength of the coupling.

At large system-bath coupling the influence action [Eq. 5] dominates over the free action, such that amplitudes for paths with $q(\tau) \neq q(\tau')$ are exponentially small in the path integral Eq. 3. In the limit $\alpha \rightarrow \infty$,

the ultra-strong coupling (USC) limit, the amplitudes for these paths vanish and only the constant path contributes, $q(\tau) = q(\tau') = q$ with $\dot{q}(\tau) = 0$. Similarly, at high temperature (but arbitrary coupling) the path length $\beta = 1/k_B T$ becomes small, so the kinetic term in the free action, $\propto \dot{q}(\tau)^2$, increasingly suppresses amplitudes for paths that deviate significantly from $q(\tau) = q$. In the limit $T \rightarrow \infty$ (zero path length) we once again find that the only relevant path is the constant path with $\dot{q}(\tau) = 0$. Thus, in either the USC limit or infinite temperature limit we have,

$$\rho(q, \eta) = \delta(\eta) Z^{-1} e^{-\beta V(q)}, \quad (8)$$

where now $Z = \int dq e^{-\beta V(q)}$. This is the same USC result obtained in [25] and is CV equivalent of the high temperature result given in [43]. Note that the argument used above to obtain the USC-MFGS is equally applicable for discrete systems. See Appendix. D for more details.

Given the discussion above, when either the coupling or temperature is large, but not infinite, we expect that only paths with small deviation around the constant path will contribute significantly to the path integral. In other words, reparameterising the path variable as $q(\tau) = q + \delta(\tau)$, we expect that only small values of $\delta(\tau)$ will be relevant to the final result. Therefore, we propose a local harmonic approximation (LHA) for $\rho(q, \eta)$, where for large coupling or temperature, the effect of the potential locally around q is effectively harmonic. Then, to second order in $\delta(\tau)$, we can write

$$\begin{aligned} V(q + \delta(\tau)) &\approx V(q) + \delta(\tau) V_1(q) + \frac{1}{2} \delta(\tau)^2 V_2(q) \\ &= V(q) - \frac{1}{2} m \omega_q^2 Q_q^2 + \frac{1}{2} m \omega_q^2 (\delta(\tau) + Q_q)^2 \end{aligned} \quad (9)$$

where

$$\omega_q = \sqrt{V_2(q)/m} \quad (10)$$

$$Q_q = \frac{V_1(q)}{V_2(q)} \quad (11)$$

are the frequency and the displacement of the effective harmonic potential, respectively, and $V_n(q)$ is the n th derivative of $V(q)$. In Fig. 1 we show the effective harmonic potentials found for different values of q using a double well potential for $V(q)$ as an example.

With Eq. 9, the path integral in Eq. 3 becomes Gaussian and can be computed exactly to obtain

$$\rho(q, \eta) = Z_R^{-1} \frac{\exp(-\beta V(q))}{\exp(-\beta \frac{1}{2} m \omega_q^2 Q_q^2)} \tilde{Z}_q \tilde{\rho}_q(Q_q, \eta) \quad (12)$$

where $\tilde{\rho}_q(Q_q, \eta)$ is the MFGS for a HO with frequency ω_q , coupled to the same bath as the original system, and \tilde{Z}_q is the corresponding partition function for the HO-bath system which depends on $V(q)$ only through the effective frequency, ω_q . We highlight that both $\tilde{\rho}_q$ and \tilde{Z}_q are

straightforward to compute since the HO-bath system is Gaussian and thus exactly solvable [45, 46]. Although we have expressed $\rho(q, \eta)$ in terms of the Gaussian state of a HO, we stress that Eq. 12 is generally not Gaussian with respect to q . This is because the potential, $V(q)$, remains completely arbitrary and all quantities on the right hand side of Eq. 12 are explicit or implicit functions of this potential.

While we have derived the LHA [Eq. 12] under the assumption of either strong coupling or large temperature, we note that it is exact for arbitrary coupling and temperature when the potential is actually harmonic, i.e. when $V(q) = aq + bq^2$ for some a and b , no matter how large $\delta(\tau)$ becomes. We therefore expect Eq. 12 to also be accurate even at weak coupling and low temperature, where $\delta(\tau)$ may not be small, as long as the third and higher derivatives of the potential are relatively small. This gives our result great flexibility in its range of validity.

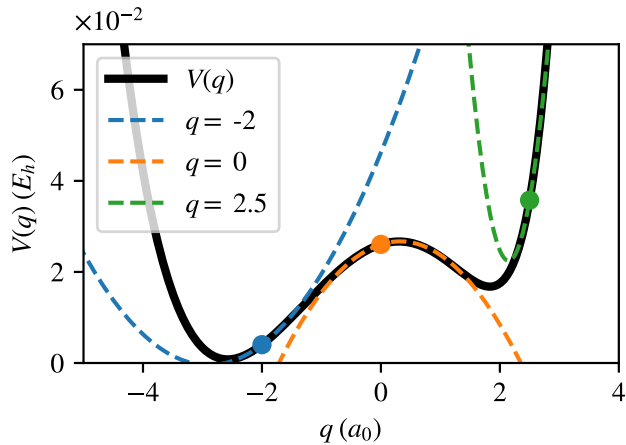


FIG. 1. Fitting a harmonic potential at each point q of a general potential $V(q)$.

One possible problem with the LHA is that when $V_2(q) < 0$, e.g., near the maxima of the potential $V(q)$, the effective frequency of the HO defined in Eq. 9 becomes imaginary, so the HO is inverted [55–57] (see the orange curve in Fig. 1). For an inverted HO, the potential is unbounded from below as $q \rightarrow \pm\infty$, so the MFGS for the HO, $\tilde{\rho}_q$ in Eq. 12, is unphysical, unnormalisable, and gives divergent observables, e.g. $\langle \hat{q}^2 \rangle = \infty$. However, we show in Appendix. B 2 that as long as $V_2(q) > -V_P$, for some $V_P > 0$, the combination $\tilde{Z}_q \tilde{\rho}_q$ can still be finite, where the quantity $\tilde{Z}_q \tilde{\rho}_q$ amounts to an unnormalised path integral which has its important contribution still coming from a finite deviation from the constant path $q(\tau) = q$, as required for LHA to work for general potentials.

This number, V_P , is given by the smallest solution of

the following equation in x ,

$$\sum_{n=1}^{\infty} \frac{x}{y_n - x} = \frac{1}{2}, \quad (13)$$

where

$$y_n = m\nu_n^2 + \int_0^{\infty} d\omega \frac{J(\omega)}{\omega} \frac{2\nu_n^2}{\omega^2 + \nu_n^2}, \quad (14)$$

and $\nu_n = 2\pi n k_B T$ are the Matsubara frequencies. Thus, provided that $V_2(q) > -V_P$, the LHA remains finite even for $V_2(q) < 0$ and then can be applied to nontrivial potentials, like the one depicted in Fig. 1. We note that in the large coupling or temperature limits we have assumed in deriving the LHA, for $x < y_1$, the $n = 1$ term in Eq. 13 dominates and we obtain the approximate solution $V_P \approx y_1/3$. Since y_n diverges with both coupling and temperature, we find the condition $V_2(q) > -V_P$ is always satisfied in this limit, consistent with LHA becoming exact there.

In order to estimate the error associated with LHA, let us first define two length scales. For the effective quadratic potential approximated at point q , let $q_{cl}(\tau)$ denote the classical path starting and ending at the point $q + \eta$ and $q - \eta$. Then, let $\Delta(q, \eta)$ denote the maximum deviation of the classical path from the constant path $q'(\tau) = q$ and let $\mathcal{E}(q)$ denote the typical quantum deviation of all the paths about $q_{cl}(\tau)$ that have significant contribution to the action. An estimate for $\Delta(q, \eta)$ and $\mathcal{E}(q)$ is derived in Appendix. C 1.

Then, the leading order correction to LHA is given by $\mathcal{T}(q, \eta)\rho(q, \eta)$, where we have,

$$\mathcal{T}(q, \eta) \equiv -\beta \frac{V_3(q)}{3!} (\Delta(q, \eta)^3 + 3\mathcal{E}(q)^2 \Delta(q, \eta)) \quad (15)$$

The relative error associated with the expectation value of an observable \hat{O} is given as [Appendix. C],

$$\epsilon_{\hat{O}} = \frac{1}{\langle \hat{O} \rangle} \int dq \int d\eta \hat{O}(q, \eta) \epsilon(q, \eta) |\rho(q, \eta)| \quad (16)$$

where, we have,

$$\epsilon(q, \eta) = |\mathcal{T}(q, \eta)| + \epsilon_T \quad (17)$$

$$\epsilon_T \equiv \int dq \rho(q) |\mathcal{T}(q)| \quad (18)$$

For LHA to be valid for the matrix element $\rho(q, \eta)$, we need $\mathcal{T}(q, \eta) \ll 1$. We also need $\epsilon_T \ll 1$, which translates into,

$$|V_3(q)| \ll \frac{3!}{\beta \rho(q) |\Delta(q)^3 + 3\mathcal{E}(q)^2 \Delta(q)|} \quad (19)$$

If, for a system, Eq. 19 is invalid in some region, this does not make LHA totally inapplicable. As an example, if it is valid in two regions of space, A and B, then LHA

can still predict the ratio of populations ρ_A/ρ_B in these two regions.

Finally, for an off-diagonal density matrix element $\rho(q, \eta)$, the value of the classical deviation, $\Delta(q, \eta)$, is at least as large as η , and hence as the value of η is increased, a stronger constraint on $V_3(q)$ is imposed in Eq. 19. This sets a limit on the length scale on which LHA can accurately capture spatial coherences.

We summarize by commenting that each term in the action in Eq. 3 gives rise to a regime in which LHA is accurate, i.e. the kinetic, dissipative and potential terms each give the high temperature, large coupling and the ‘slowly varying potential’ limit, respectively.

III. APPLICATION

A. Quartic Oscillator

We are now going to use LHA to study various CV systems. Let us first study a quartic oscillator whose potential is given by,

$$V(q) = \frac{1}{2}m\omega^2q^2 + aq^4 \quad (20)$$

A quartic potential is the simplest bounded potential that provides a deviation from the quadratic HO potential, latter being the case for which LHA works exactly. A quartic oscillator has been studied in the context of quantum to classical transition [24], quantum chaos [14–16] and as a model of bath oscillators interacting with a system [58]. Here, we study how the non-Gaussianity that naturally emerges in the MFGS of a quartic oscillator changes as the system bath coupling is increased.

We use an Ohmic spectral density of exponential cutoff form (as some integrals required to do the TEMPO calculations done in this section are analytically known in this cutoff),

$$J(\omega) = \frac{2m\gamma}{\pi} \omega \exp\left(-\frac{\omega}{\Omega}\right) \quad (21)$$

Using Hartree atomic units, we set $\omega = 1E_h$, $\Omega = 5E_h$, $m = 1m_e$ and $k_B T = 0.5E_h$.

To characterize the MFGS, we calculate the second and fourth order cumulants of position, i.e. $\kappa_2 = \langle q^2 \rangle$ and $\kappa_4 = \langle q^4 \rangle - 3\langle q^2 \rangle^2$, respectively. The former of these quantifies the width of the spatial probability density while the latter quantifies how non-Gaussian the state is, since all cumulants of order three and higher vanish for Gaussian states. The system is symmetric around $q = 0$ so the odd-order cumulants of q vanish identically, regardless of whether the state is Gaussian.

To benchmark our results we use the analytically known weak and USC results, as well as the numerically exact method, TEMPO [47–49], applicable in weak and intermediate coupling regime.

The TEMPO is a tensor network technique to efficiently evaluate the path integral given in Eq. 3. It has

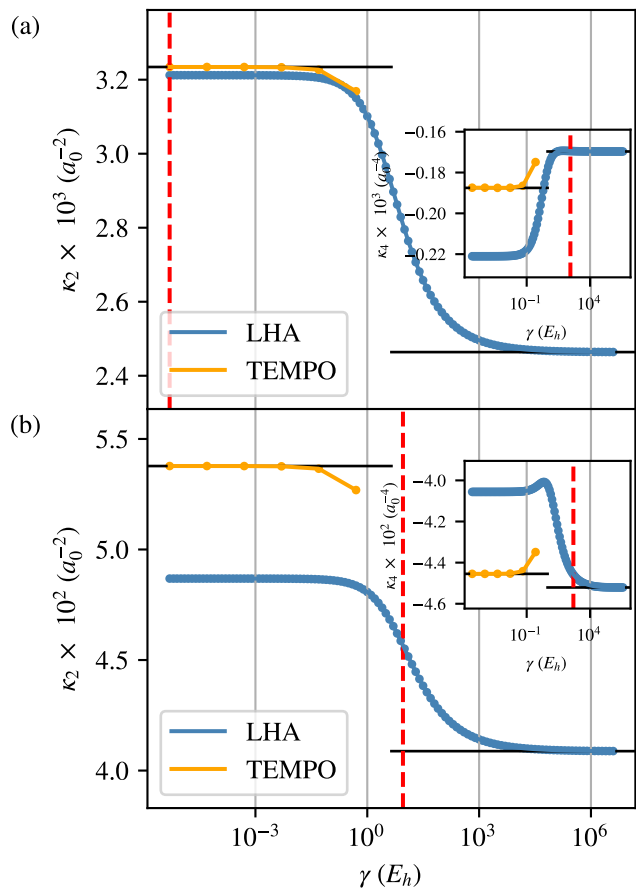


FIG. 2. The 2nd and 4th cumulant as a function of the system-bath coupling parameter, γ , for anharmonicity (a) $a = 2.5 \times 10^{-3} (E_h/a_0^4)$ and (b) $a = 5 \times 10^{-2} (E_h/a_0^4)$. Orange and blue curves indicate results obtained using TEMPO and LHA, respectively, while the horizontal black lines indicate the exact results for $\gamma = 0$ and $\gamma = \infty$. The vertical dashed line corresponds to the point to the right of which $\epsilon_{\kappa_{2/4}} < 0.1$ [Eq. 22, Eq. 23]. Convergence for TEMPO calculations for both (a) and (b) at $\gamma = 0.5 E_h$ was observed for the number of path integral timesteps equal to 60, the system truncation dimension of 9, and the TEMPO SVD precision parameter of 10^{-9} .

been previously used to calculate the MFGS for discrete systems [47]. Here we use it to study a CV system like a particle in a generic 1D potential $V(q)$. Although the system in question is infinite dimensional, at any given temperature and coupling, it can be approximated as an effectively finite dimensional system by truncating the system Hilbert space in the energy eigenbasis [54]. The value of this effective dimension can be determined through a convergence test. In this case for example, for $\gamma = 0.5 E_h$, we needed to treat the system as an effectively 9 dimensional discrete system to get sufficient convergence.

Figure 2 (a) and (b) plot both the cumulants, κ_2 and κ_4 , calculated using LHA, as a function of coupling

strength for $a = 2.5 \times 10^{-3}$ and 5×10^{-2} [Eq. 20], respectively. The vertical red line marks the value of γ such that for γ larger than this, the associated relative error $\epsilon_{\kappa_2}, \epsilon_{\kappa_4} < 0.1$, where, from Eq. 16 we have,

$$\epsilon_{\kappa_2} = \epsilon_{\hat{q}^2} \quad (22)$$

$$\epsilon_{\kappa_4} = \frac{\langle \hat{q}^4 \rangle \epsilon_{\hat{q}^4} + 6 \langle \hat{q}^2 \rangle \epsilon_{\hat{q}^2}}{\kappa_4} \quad (23)$$

As expected, the accuracy of LHA falls as the value of γ is decreased from infinity while for TEMPO, the computational resources required increase as the value of γ is increased from the weak coupling regime. Because of computational constraints, here we only show the TEMPO results up to $\gamma \leq 0.5$. In Figure 2 (b), we observe a nontrivial rise in the TEMPO curve for κ_4 as γ is increased, followed by an eventual decay to the USC value as suggested by the LHA curve, suggesting a peak at about $\gamma = 10$.

The results for MFGS in weak and USC limit in Figure 2 (a) and (b) suggests that the non-gaussianity, that naturally emerges in a quartic oscillator, may either get enhanced or decay as γ is increased, depending on the value of the parameter a used in the potential $V(q)$ [Eq. 20]. TEMPO and LHA complement each other to calculate the γ dependence of κ_4 in the low and high γ limit, respectively. Note that non-Gaussianity is considered a resource for quantum information processing in CV systems [8, 59], and LHA and TEMPO can help quantify how the non-Gaussianity depends upon the system-bath coupling strength for a CV system.

B. Asymmetric double well potential

Let us now discuss an asymmetric quartic DW potential of the form,

$$V(q) = a_4 q^4 - a_2 q^2 + a_1 q \quad (24)$$

where we set $a_4 = 1/2 = a_2$. In this and following sections, we use an ohmic spectral density of Drude-Lorentz form,

$$J(\omega) = \frac{2m\gamma}{\pi} \omega \frac{\Omega^2}{\omega^2 + \Omega^2} \quad (25)$$

as this form of spectral density admits a closed form expression for the LHA [46]. We again set $\omega = 1E_h$, $\Omega = 5E_h$, $m = 1m_e$ and $k_B T = 0.5E_h$.

As the accuracy of LHA increases with increasing system bath coupling, we will instead test its applicability in weak coupling limit. At $\gamma = 0$, we are interested in the LHA value of the probability, \mathcal{P} , of finding the particle in the right well, given as,

$$\mathcal{P} = \int_{q_b}^{\infty} \rho(q) dq \quad (26)$$

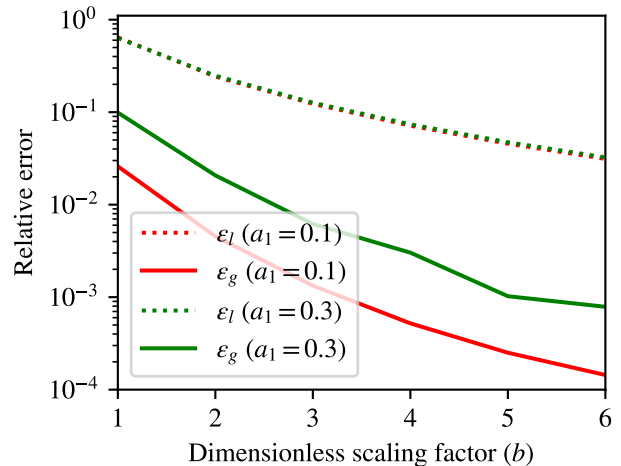


FIG. 3. Plot for relative error (solid lines) [Eq. 28] for LHA value of the Gibbs state probability \mathcal{P} [Eq. 26] for the particle to be found in the right well of an asymmetric double well potential $\bar{V}_b(q)$ [Eq. 27], as a function of b , a dimensionless parameter of $\bar{V}_b(q)$. The dotted lines represent the estimated relative error for the same [Eq. 16]. Plots are for $a_1 = 0.1$ (red lines) and 0.3 (green lines), where a_1 quantifies the degree of asymmetry in $\bar{V}_b(q)$. Note that both the dotted lines are almost overlapping.

where, q_b represents the position of the peak of the barrier. We also want to verify the associated estimated relative error for LHA [Eq. 16] against the analytically derivable value for the same at $\gamma = 0$.

Since LHA will work at lower coupling only if $V(q)$ varies slowly, let us define,

$$\bar{V}_b(q) \equiv b \times V(q/b) \quad (27)$$

where for a fixed value of $b > 1$, $\bar{V}_b(q)$ is just a new rescaled potential with smaller values for the higher derivatives with respect to q . Note that $\bar{V}_b(q)$ has been mathematically constructed just to verify the validity of the error estimate [Eq. 16].

At a given value of b , let ρ_b represent the LHA state and $\sigma_b = Z_b^{-1} \exp\{-\beta H_0\}$ represent the Gibbs state with $\mathcal{P}_l(b)$ and $\mathcal{P}_g(b)$ being the corresponding values of the probability of finding the particle in the right well, respectively. Here, Z_b is an appropriate normalization factor. Then, let the estimated and analytical value of the relative error be denoted as $\epsilon_l(b)$ [Eq. 16] and $\epsilon_g(b)$, respectively, where $\epsilon_g(b)$ is defined as,

$$\epsilon_g(b) = \frac{|\mathcal{P}_l(b) - \mathcal{P}_g(b)|}{\mathcal{P}_g(b)} \quad (28)$$

In Figure 3, we plot $\epsilon_l(b)$ and $\epsilon_g(b)$ as a function of b for $a_1 = 0.1$ and 0.3 [Eq. 24]. As expected, as the value of b increases and the potential becomes smoother, both $\epsilon_l(b)$ and $\epsilon_g(b)$ decrease in value. We find that $\epsilon_l(b)$ provides an upper bound on $\epsilon_g(b)$, roughly overestimating it by

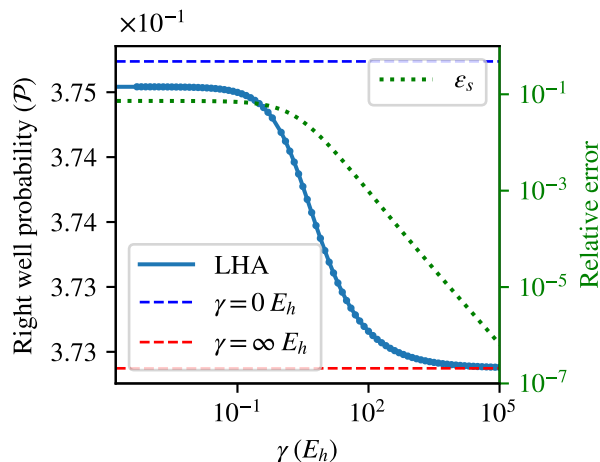


FIG. 4. The left y-axis plots the LHA value for the probability \mathcal{P} (solid blue line) for a particle in an asymmetric double well potential $\bar{V}_b(q)$ [Eq. 27] to be found in the right well [Eq. 26], as a function of coupling parameter γ , for $b = 4$. The dashed blue and red lines mark the value of \mathcal{P} corresponding to $\gamma = 0$ and ∞ , respectively. The right y-axis plots the estimated relative error for the corresponding value of \mathcal{P} [Eq. 16].

about two orders of magnitude in this case. One possible explanation for this could be that the actual error associated with the expectation value of an observable \hat{O} can get canceled out during the act of taking the trace, $\text{Tr}(\hat{O}\rho)$.

In Figure 4, we fix $b = 4$ and plot $\mathcal{P}_l(b = 4)$ as a function of γ . We note that throughout the range of γ , the relative error, ϵ_l , is always less than or equal to 0.07, indicating that LHA can accurately calculate the value of \mathcal{P} for this DW system throughout the range of the coupling parameter. Note that for this DW system, the values for the distance between the wells, the barrier height from the potential minima and the energy difference between the well minimas are given as $5.6a_0$, $0.81E_h$ and $0.56E_h$, respectively. Hence, although these parameters are not extreme, yet we note that this DW potential was constructed to be slowly varying with respect to q so that LHA would give accurate results for it, and hence at best, provides an evidence for the accuracy of LHA when $V(q)$ varies slowly.

On the right y-axis of Figure 4, we plot the relative error estimate $\epsilon_l(\gamma)$. We note that, as expected, $\epsilon_l(\gamma)$ monotonically decreases with increasing value of γ . Note that for $\gamma \lesssim 0.1E_h$, the value of $\epsilon_l(\gamma)$ plateaus, suggesting that in low γ limit, the kinetic term in the action [Eq. 3] dominates over the dissipative term, and is the sole (γ independent) factor that is still responsible for the accuracy of LHA.

C. Proton tunneling in DNA

Slocombe et al. [36, 37] performed an open quantum system analysis of a proton in Guanine-Cytosine (G-C) pair in DNA to study the probability for it to tunnel to a mutated state. They treated the problem as a particle in an asymmetric double well potential $V(q)$ (see Figure 1), interacting with a non-interacting bosonic bath through an Ohmic spectral density [Eq. 25]. Here, $V(q)$ is taken to be a back-to-back Morse potential,

$$V(q) = v_1 \left(e^{-2a_1(q-r_1)} - 2e^{-a_1(q-r_1)} \right) + v_2 \left(e^{-2a_2(r_2-q)} - 2e^{-a_2(r_2-q)} \right) \quad (29)$$

where the lower and higher well represent the canonical and mutated state for the proton to be in, respectively. Here, in Hartree atomic units, $v_1 = 0.1617E_h$, $v_2 = 0.082E_h$, $a_1 = 0.305a_0^{-1}$, $a_2 = 0.755a_0^{-1}$, $r_1 = -2.7a_0$ and $r_2 = 2.1a_0$. The parameters of the spectral density [Eq. 25] was taken to be, $\gamma = 0.018E_h \equiv \gamma_p$ and $k_B T = 0.00095E_h$ while an infinite bath cutoff was assumed as a Markovian approximation (i.e., $\Omega = \infty E_h$) [37]. Here, γ_p denotes the biologically relevant value of γ for this system. They calculated the steady state for this system using Caldeira Leggett master equation (CLME) and found the probability for the proton to tunnel to the mutated state, defined as

$$\mathcal{M} = \int_{q_b}^{\infty} \rho(q) dq \quad (30)$$

to be of the order of 10^{-4} , which, as a point of comparison, is several orders of magnitude higher than the zero coupling value of about 2.7×10^{-8} . Here q_b denotes the position of the barrier maxima.

We remark that CLME is a weak coupling master equation, which requires $\gamma_p \ll K_B T, \Omega$. But, for this system, $\gamma_p > K_B T$ and hence the system is well outside the weak coupling regime. This motivates us to study the MFGS of this system using LHA.

In Figure 5, we plot LHA value for \mathcal{M} as a function of γ along with the estimated relative error, $\epsilon_{\mathcal{M}}$ [Eq. 16],

$$\epsilon_{\mathcal{M}} = \frac{1}{\mathcal{M}} \int_{q_b}^{\infty} \epsilon(q) \rho(q) dq \quad (31)$$

We note that at $\gamma = \gamma_p$, $\epsilon_{\mathcal{M}} \approx 0.19$. while for $\gamma \geq 10\gamma_p$, $\epsilon_{\mathcal{M}} \ll 1$. Hence, in the region where LHA is applicable ($\gamma \geq 10\gamma_p$), as the value of γ is lowered from infinity, we see the value of \mathcal{M} reducing from the USC value, suggesting that $\mathcal{M} = 10^{-4}$ is unlikely. But at $\gamma = \gamma_p$, we can't speculate on the true value of \mathcal{M} since the error is high.

This disagreement could have a couple of possible reasons. Note that in the intermediate coupling regime, as in this case, it is still unclear whether MFGS is actually the steady state of the system or not [25, 60]. On

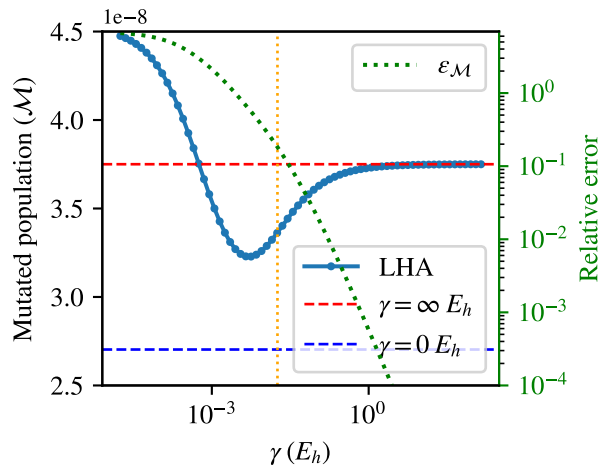


FIG. 5. Left y-axis plots the LHA value for mutation probability of the proton, \mathcal{M} (solid blue line), as a function of the coupling parameter γ . The dashed blue and red lines mark the value of \mathcal{M} corresponding to $\gamma = 0$ and ∞ , respectively. The vertical orange dotted line marks $\gamma_p = 0.018 E_h$ (the biologically relevant value of γ). The green dotted curve corresponding to the right hand side y-axis quantifies the estimated relative error ($\epsilon_{\mathcal{M}}$ [Eq. 31]) in the LHA value for \mathcal{M} .

the other hand, CLME, being a weak coupling master equation, could be responsible for this disagreement.

Figure 6 presents a plot of \mathcal{M} as a function of temperature T , across a temperature range of approximately $300K \pm 20\%$. As expected, we find that \mathcal{M} rises roughly exponentially with the value of T . We also plot the value of \mathcal{M} corresponding to $\gamma = 0$ and $\gamma = \infty$, finding it to closely follow the same trend. At the temperature of about $87^\circ C$, we find an approximately 10 times rise in the value of \mathcal{M} as compared with corresponding room temperature value. The accuracy of LHA is observed to increase with a rise in temperature, as expected [Appendix. D 2], as observed from the decay in the plot for the relative error $\epsilon_{\mathcal{M}}$ with increasing temperature.

IV. CONCLUSION

For a particle in a 1D potential $V(q)$, we derived an approximate expression for the MFGS [Eq. 1]. This method is accurate when either the system-bath coupling or the temperature is large, or when the third and higher derivatives of the potential are small compared to certain system-bath specific parameters. This result thus has applications in a wide variety of problems in quan-

tum thermodynamics, technology, chemistry and quantum biology.

We have found that for a CV system, the USC [25] and high temperature [43] results obtained recently are a special case of LHA [Eq. 12]. As a future direction, it would be interesting to apply a similar approach to use the ana-

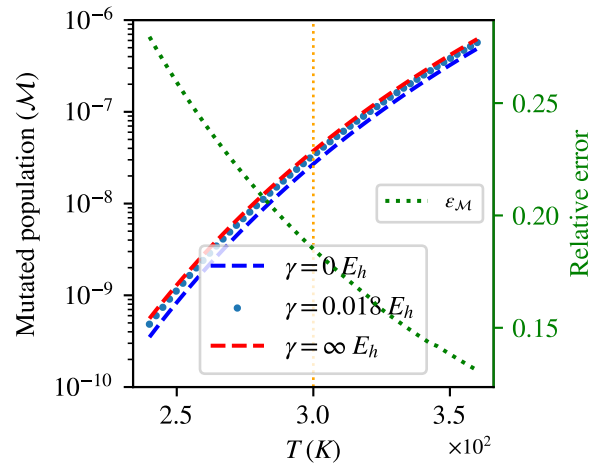


FIG. 6. Left y-axis plots the LHA value for the mutation probability, \mathcal{M} , as a function of temperature T (in Kelvin) for biologically relevant value of the coupling parameter ($\gamma_p = 0.018 E_h$) (blue scatter points). The dashed blue and red lines mark the value of \mathcal{M} corresponding to $\gamma = 0$ and ∞ , respectively. The vertical orange dotted line marks $T = 300K$ (i.e., room temperature). The green dotted curve corresponding to the right hand side y-axis quantifies the estimated relative error ($\epsilon_{\mathcal{M}}$ [Eq. 31]) in the LHA value for \mathcal{M} .

lytically known exact expression for the master equation for a harmonic oscillator [61] to derive an approximate master equation for a particle in generic potential $V(q)$. Moreover, determining the origin of mismatch between MFGS and the steady state expression for the mutated population \mathcal{M} for the proton tunneling problem considered in Sec. III C will be of interest [36].

Finally, different ways to improve on LHA and get better error bounds for it will enhance its applicability to physical problems.

V. ACKNOWLEDGEMENT

I would like to thank my PhD supervisor, Dr. Sibasis Ghosh, for his comments, suggestions and several extended discussions. I also thank Aidan Strathearn, who has contributed significantly to the preparation of this manuscript.

[1] S. L. Braunstein and P. Van Loock, “Quantum information with continuous variables,” *Reviews of modern*

physics, vol. 77, no. 2, p. 513, 2005.

- [2] T. Ralph, “Quantum optical systems for the implementation of quantum information processing,” *Reports on Progress in Physics*, vol. 69, pp. 853 – 898, 2006.
- [3] I. Djordjevic, “Hybrid cv-dv quantum communications and quantum networks,” *IEEE Access*, vol. 10, pp. 23 284–23 292, 2022.
- [4] A. Inoue, T. Kashiwazaki, T. Yamashima, N. Takanashi, T. Kazama, K. Enbutsu, K. Watanabe, T. Umeki, M. Endo, and A. Furusawa, “Toward a multi-core ultrafast optical quantum processor: 43-ghz bandwidth real-time amplitude measurement of 5-db squeezed light using modularized optical parametric amplifier with 5g technology,” *Applied Physics Letters*, 2022.
- [5] X. Yang and M. Xiao, “Electromagnetically induced entanglement,” *Scientific Reports*, vol. 5, 2015.
- [6] C. Gross, H. Strobel, E. Nicklas, T. Zibold, N. Bar-Gill, G. Kurizki, and M. Oberthaler, “Atomic homodyne detection of continuous-variable entangled twin-atom states,” *Nature*, vol. 480, pp. 219–223, 2011.
- [7] J. Huang, Y. Liu, J.-F. Huang, and J. Liao, “Generation of macroscopic entangled cat states in a longitudinally coupled cavity-qed model,” *Physical Review A*, 2019.
- [8] R. Takagi and Q. Zhuang, “Convex resource theory of non-gaussianity,” *Physical Review A*, 2018.
- [9] G. Ferrari, L. Lami, T. Theurer, and M. Plenio, “Asymptotic state transformations of continuous variable resources,” *Communications in Mathematical Physics*, vol. 398, pp. 291 – 351, 2020.
- [10] V. Narasimhachar, S. Assad, F. Binder, J. Thompson, B. Yadin, and M. Gu, “Thermodynamic resources in continuous-variable quantum systems,” *npj Quantum Information*, vol. 7, pp. 1–7, 2019.
- [11] E. Hoskinson, F. Lecocq, N. Didier, A. Fay, F. Hekking, W. Guichard, O. Buisson, R. Dolata, B. Mackrodt, and A. Zorin, “Quantum dynamics in a camelback potential of a dc squid,” *Physical review letters*, vol. 102 9, p. 097004, 2008.
- [12] R. Ferreira and G. Bastard, “Tunnelling and relaxation in semiconductor double quantum wells,” *Reports on Progress in Physics*, vol. 60, pp. 345–387, 1997.
- [13] Monteoliva and Paz, “Decoherence and the rate of entropy production in chaotic quantum systems,” *Physical review letters*, vol. 85 16, pp. 3373–6, 2000.
- [14] B.C.Bag, S.Chaudhuri, J. Chaudhuri, and D.S.Ray, “A semiclassical theory of quantum noise in open chaotic systems,” *Physica D: Nonlinear Phenomena*, vol. 125, pp. 47–64, 1998.
- [15] A. Jt, “Semiclassical chaos in quartic anharmonic oscillators,” *Physical Review A*, vol. 45, pp. 5373–5377, 1992.
- [16] B. Chakrabarty and S. Chaudhuri, “Out of time ordered effective dynamics of a quartic oscillator,” *SciPost Physics*, 2019.
- [17] K.-L. Liu and H. Goan, “Non-markovian entanglement dynamics of quantum continuous variable systems in thermal environments,” *Physical Review A*, vol. 76, p. 022312, 2007.
- [18] R. Vasile, S. Maniscalco, M. Paris, H. Breuer, and J. Piilo, “Quantifying non-markovianity of continuous-variable gaussian dynamical maps,” *Physical Review A*, vol. 84, p. 052118, 2011.
- [19] C. Hörhammer and H. Buettner, “Environment-induced two-mode entanglement in quantum brownian motion,” *Physical Review A*, vol. 77, p. 042305, 2007.
- [20] J. Ruostekoski and D. F. Walls, “Bose-einstein condensate in a double-well potential as an open quantum system,” *Physical Review A*, vol. 58, no. 1, p. R50, 1998.
- [21] M. P. Fisher and A. T. Dorsey, “Dissipative quantum tunneling in a biased double-well system at finite temperatures,” *Physical review letters*, vol. 54, no. 15, p. 1609, 1985.
- [22] H. Grabert and U. Weiss, “Quantum tunneling rates for asymmetric double-well systems with ohmic dissipation,” *Physical review letters*, vol. 54, no. 15, p. 1605, 1985.
- [23] M. Topaler and N. Makri, “Quantum rates for a double well coupled to a dissipative bath: Accurate path integral results and comparison with approximate theories,” *The Journal of chemical physics*, vol. 101, no. 9, pp. 7500–7519, 1994.
- [24] A. C. Oliveira, J. G. P. de Faria, and M. Nemes, “Quantum-classical transition of the open quartic oscillator: The role of the environment,” *Physical review. E, Statistical, nonlinear, and soft matter physics*, vol. 73 4 Pt 2, p. 046207, 2006.
- [25] J. Cresser and J. Anders, “Weak and ultrastrong coupling limits of the quantum mean force gibbs state,” *Physical Review Letters*, vol. 127, no. 25, p. 250601, 2021.
- [26] U. Seifert, “First and second law of thermodynamics at strong coupling,” *Physical review letters*, vol. 116, no. 2, p. 020601, 2016.
- [27] T. G. Philbin and J. Anders, “Thermal energies of classical and quantum damped oscillators coupled to reservoirs,” *Journal of Physics A: Mathematical and Theoretical*, vol. 49, no. 21, p. 215303, 2016.
- [28] C. Jarzynski, “Nonequilibrium work theorem for a system strongly coupled to a thermal environment,” *Journal of Statistical Mechanics: Theory and Experiment*, vol. 2004, no. 09, p. P09005, 2004.
- [29] M. Campisi, P. Talkner, and P. Hänggi, “Fluctuation theorem for arbitrary open quantum systems,” *Physical review letters*, vol. 102, no. 21, p. 210401, 2009.
- [30] T. W. Allen, O. S. Andersen, and B. Roux, “Molecular dynamics—potential of mean force calculations as a tool for understanding ion permeation and selectivity in narrow channels,” *Biophysical chemistry*, vol. 124, no. 3, pp. 251–267, 2006.
- [31] K. Maksimiak, S. Rodziewicz-Motowidło, C. Czaplowski, A. Liwo, and H. A. Scheraga, “Molecular simulation study of the potentials of mean force for the interactions between models of like-charged and between charged and nonpolar amino acid side chains in water,” *The Journal of Physical Chemistry B*, vol. 107, no. 48, pp. 13 496–13 504, 2003.
- [32] B. Roux and T. Simonson, “Implicit solvent models,” *Biophysical chemistry*, vol. 78, no. 1-2, pp. 1–20, 1999.
- [33] B. Roux, “The calculation of the potential of mean force using computer simulations,” *Computer physics communications*, vol. 91, no. 1-3, pp. 275–282, 1995.
- [34] M. Gillan, “Quantum-classical crossover of the transition rate in the damped double well,” *Journal of Physics C: Solid State Physics*, vol. 20, no. 24, p. 3621, 1987.
- [35] Y. Liu, Y. Yan, T. Xing, and Q. Shi, “Understanding the large kinetic isotope effect of hydrogen tunneling in condensed phases by using double-well model systems,” *The Journal of Physical Chemistry B*, vol. 125, no. 22, pp. 5959–5970, 2021.
- [36] L. Slocombe, M. Sacchi, and J. Al-Khalili, “An open quantum systems approach to proton tunnelling in dna,”

- Communications Physics*, vol. 5, no. 1, p. 109, 2022.
- [37] L. Slocombe, “Quantum effects in dna replication fidelity,” Ph.D. dissertation, University of Surrey, 2022.
- [38] J. Zhang, R. Borrelli, and Y. Tanimura, “Proton tunneling in a two-dimensional potential energy surface with a non-linear system–bath interaction: Thermal suppression of reaction rate,” *The Journal of Chemical Physics*, vol. 152, no. 21, 2020.
- [39] J. P. Bothma, J. B. Gilmore, and R. H. McKenzie, “The role of quantum effects in proton transfer reactions in enzymes: quantum tunneling in a noisy environment?” *New Journal of Physics*, vol. 12, no. 5, p. 055002, 2010.
- [40] H. P. Breuer and F. Petruccione, *The theory of open quantum systems*. Great Clarendon Street: Oxford University Press, 2002.
- [41] A. Trushechkin, “Quantum master equations and steady states for the ultrastrong-coupling limit and the strong-decoherence limit,” *Physical Review A*, vol. 106, no. 4, p. 042209, 2022.
- [42] C. L. Latune, “Steady state in ultrastrong coupling regime: perturbative expansion and first orders,” *arXiv preprint arXiv:2110.02186*, 2021.
- [43] G. Timofeev and A. Trushechkin, “Hamiltonian of mean force in the weak-coupling and high-temperature approximations and refined quantum master equations,” *International Journal of Modern Physics A*, vol. 37, no. 20n21, p. 2243021, 2022.
- [44] A. Gelzinis and L. Valkunas, “Analytical derivation of equilibrium state for open quantum system,” *The Journal of Chemical Physics*, vol. 152, no. 5, 2020.
- [45] H. Grabert, P. Schramm, and G.-L. Ingold, “Quantum brownian motion: The functional integral approach,” *Physics reports*, vol. 168, no. 3, pp. 115–207, 1988.
- [46] U. Weiss, *Quantum dissipative systems*. World Scientific, 2012.
- [47] Y.-F. Chiu, A. Strathearn, and J. Keeling, “Numerical evaluation and robustness of the quantum mean-force gibbs state,” *Physical Review A*, vol. 106, no. 1, p. 012204, 2022.
- [48] A. Strathearn, P. Kirton, D. Kilda, J. Keeling, and B. W. Lovett, “Efficient non-markovian quantum dynamics using time-evolving matrix product operators,” *Nature communications*, vol. 9, no. 1, p. 3322, 2018.
- [49] A. Strathearn, *Modelling non-Markovian quantum systems using tensor networks*. Springer Nature, 2020.
- [50] R. P. Feynman and F. Vernon Jr, “The theory of a general quantum system interacting with a linear dissipative system,” *Annals of physics*, vol. 281, no. 1-2, pp. 547–607, 2000.
- [51] N. Makri and D. E. Makarov, “Tensor propagator for iterative quantum time evolution of reduced density matrices. i. theory,” *The Journal of chemical physics*, vol. 102, no. 11, pp. 4600–4610, 1995.
- [52] —, “Tensor propagator for iterative quantum time evolution of reduced density matrices. ii. numerical methodology,” *The Journal of chemical physics*, vol. 102, no. 11, pp. 4611–4618, 1995.
- [53] Y. Tanimura, “Numerically “exact” approach to open quantum dynamics: The hierarchical equations of motion (heom),” *The Journal of chemical physics*, vol. 153, no. 2, 2020.
- [54] M. Topaler and N. Makri, “System-specific discrete variable representations for path integral calculations with quasi-adiabatic propagators,” *Chemical physics letters*, vol. 210, no. 4-6, pp. 448–457, 1993.
- [55] G. Barton, “Quantum mechanics of the inverted oscillator potential,” *Annals of Physics*, vol. 166, no. 2, pp. 322–363, 1986.
- [56] V. Subramanyan, S. S. Hegde, S. Vishveshwara, and B. Bradlyn, “Physics of the inverted harmonic oscillator: From the lowest landau level to event horizons,” *Annals of Physics*, vol. 435, p. 168470, 2021.
- [57] S. Baskoutas, A. Jannussis, and R. Mignani, “Quantum tunnelling of a damped and driven, inverted harmonic oscillator,” *Journal of Physics A: Mathematical and General*, vol. 26, no. 23, p. 7137, 1993.
- [58] V. Montenegro, A. Ferraro, and S. Bose, “Nonlinearity induced entanglement stability in a qubit-oscillator system,” *Physical Review A*, vol. 90, p. 013829, 2014.
- [59] C. Weedbrook, S. Pirandola, R. García-Patrón, N. J. Cerf, T. C. Ralph, J. H. Shapiro, and S. Lloyd, “Gaussian quantum information,” *Reviews of Modern Physics*, vol. 84, no. 2, p. 621, 2012.
- [60] A. Trushechkin, M. Merkli, J. Cresser, and J. Anders, “Open quantum system dynamics and the mean force gibbs state,” *AVS Quantum Science*, vol. 4, no. 1, 2022.
- [61] B. L. Hu, J. P. Paz, and Y. Zhang, “Quantum brownian motion in a general environment: Exact master equation with nonlocal dissipation and colored noise,” *Physical Review D*, vol. 45, no. 8, p. 2843, 1992.
- [62] R. Feynman and A. Hibbs, “The path integral formulation of quantum mechanics,” *McGraw-Hill, New York*, 1965.
- [63] W. Sherman, “Summation of harmonics with random phase angles,” in *Proceedings of the Institution of Electrical Engineers*, vol. 119, no. 11. IET, 1972, pp. 1643–1648.

A. SUMMARY OF MAIN RESULTS

In this section, we will summarize the basic results of this paper. For details, see the sections mentioned here. The path integral representation for the MFGS, $\rho(q, \eta) = \langle q + \eta | \hat{\rho} | q - \eta \rangle$, is given as,

$$\rho(q, \eta) = Z_R^{-1} \int_{q+\eta}^{q-\eta} \mathcal{D}q(\tau) e^{-S[q(\tau)]} \quad (32)$$

Parameterising the path variable in terms of its deviation from the constant path, $q(\tau) = q + \delta(\tau)$, we expand the potential to second order in δ [Eq. 9], resulting in Eq. 32 becoming,

$$\rho(q, \eta) = Z_R^{-1} \exp\left(-\beta V(q) + \beta \frac{1}{2} m \omega_q^2 Q_q^2\right) \int_{\eta}^{-\eta} \mathcal{D}\delta(\tau) e^{-S_q[\delta(\tau) + Q_q]} \quad (33)$$

where $S_q[\delta(\tau) + Q_q]$ is the action for a HO with frequency ω_q [Eq. 10]. Reparametrize $\delta(\tau) + Q_q \rightarrow \delta(\tau)$ to get,

$$\int_{\eta}^{-\eta} \mathcal{D}\delta(\tau) e^{-S_q[\delta(\tau) + Q_q]} = \int_{Q_q+\eta}^{Q_q-\eta} \mathcal{D}\delta(\tau) e^{-S_q[\delta(\tau)]} \quad (34)$$

$$= \tilde{Z}_q \tilde{\rho}_q(Q_q, \eta) \quad (35)$$

where, $\tilde{\rho}_q(q, \eta)$ is the MFGS for a HO with frequency ω_q . That is, the functional integral in this equation is identical to that of a HO but for the reduced HO partition function \tilde{Z}_q . This leads us to [Eq. 12],

$$\rho(q, \eta) = Z_R^{-1} \frac{\exp(-\beta V(q))}{\exp(-\beta \frac{1}{2} m \omega_q^2 Q_q^2)} \tilde{Z}_q \tilde{\rho}_q(Q_q, \eta) \quad (36)$$

We can write the expression for LHA more explicitly as,

$$\rho(q, \eta) = Z^{-1} \mathcal{G}(q) \exp\left(-\frac{1}{2 \langle \hat{X}^2(q) \rangle} \left(\frac{V_1(q)}{V_2(q)}\right)^2 - 2 \langle \hat{P}^2(q) \rangle \eta^2 - \beta \left(V(q) - \frac{V_1(q)^2}{2V_2(q)}\right)\right) \quad (37)$$

Here, $\langle \hat{X}^2(q) \rangle$ and $\langle \hat{P}^2(q) \rangle$ are the corresponding effective $\langle \hat{q}^2 \rangle$ and $\langle \hat{p}^2 \rangle$ values of the harmonic potential approximated at point q , whose value is given as [45, 46],

$$\langle \hat{X}^2(q) \rangle = \frac{1}{m\beta} \sum_{n=-\infty}^{+\infty} \frac{1}{\mathcal{A}_n(q)} \quad (38)$$

$$\langle \hat{P}^2(q) \rangle = \frac{m}{\beta} \sum_{n=-\infty}^{+\infty} \frac{\omega_q^2 + \zeta_n}{\mathcal{A}_n(q)} \quad (39)$$

$$\mathcal{A}_n(q) = \omega_q^2 + \nu_n^2 + \zeta_n \quad (40)$$

$$\nu_n \equiv 2\pi n k_B T \quad (41)$$

$$\zeta_n \equiv \frac{1}{m} \int_0^\infty d\omega' \frac{J(\omega')}{\omega'} \frac{2\nu_n^2}{\omega'^2 + \nu_n^2} \quad (42)$$

To arrive at Eq. 37, we did the following replacement in Eq. 36. The expression for the reduced partition function, \tilde{Z}_q , is given as [Appendix. B1],

$$\tilde{Z}_q = \mathcal{I}(q) \sqrt{2\pi \langle \hat{X}^2(q) \rangle} \quad (43)$$

where $\mathcal{I}(q)$ is defined as,

$$\mathcal{I}(q) \equiv \int_0^0 \mathcal{D}\delta(\tau) e^{-S_q[\delta(\tau)]} \quad (44)$$

$$= \frac{Z_R}{Z} \mathcal{G}(q) \quad (45)$$

Here, Z [Eq. 37] is an appropriate constant independent of q , and hence is a normalization factor common for all the effective quadratic approximations done at all points q . This would imply, for example, that Z can depend upon $k_B T$, Ω and γ but not on ω_q because the latter explicitly depends upon $V(q)$ by definition [Eq. 10]. The non-trivial part is to then show that $\mathcal{G}(q)$ is given as [Appendix. B 2],

$$\mathcal{G}(q) = \frac{1}{\sqrt{m\omega_q^2\beta\langle\hat{X}^2(q)\rangle}} \prod_{n=1}^{\infty} \frac{\nu_n^2 + \zeta_n}{\mathcal{A}_n(q)} \quad (46)$$

Furthermore, the expression for $\tilde{\rho}_q(q, \eta)$ is given as [45, 46],

$$\tilde{\rho}_q(q, \eta) = \frac{1}{\sqrt{2\pi\langle\hat{X}^2(q)\rangle}} \exp\left(-\frac{q^2}{2\langle\hat{X}^2(q)\rangle} - 2\langle\hat{P}^2(q)\rangle\eta^2\right) \quad (47)$$

With these replacements, we can move from Eq. 36 to Eq. 37. We note that, for a specific spectral density, like Ohmic spectral density with Drude-Lorentz cutoff [Eq. 25], the expressions for Eq. 38, Eq. 39 and Eq. 46 can be evaluated in closed form [46].

Note that when $\omega_q^2 < 0$, $\langle\hat{X}^2(q)\rangle$ and $\langle\hat{P}^2(q)\rangle$, as defined in Eq. 38 and Eq. 39, can no more be interpreted as expectation values $\langle\hat{q}^2\rangle$ and $\langle\hat{p}^2\rangle$ for the corresponding inverted HO, and must instead be taken as mathematical objects as defined above. In Appendix. B 2, we show that as long as

$$m\omega_q^2 > -V_P \quad (48)$$

where V_P is defined in Sec. II, the unnormalized path integral for an inverted HO,

$$\tilde{Z}_q \tilde{\rho}_q(Q_q, \eta) = \int_{Q_q+\eta}^{Q_q-\eta} \mathcal{D}\delta(\tau) e^{-S_q[\delta(\tau)]} \quad (49)$$

is still convergent, which is what we require in the expression of LHA [Eq. 36]. We note here that $\tilde{\rho}_q(Q_q, \eta)$ and \tilde{Z}_q are both individually undefined for any inverted HO, regardless of Eq. 48. Given Eq. 48, to show that Eq. 49 converges, it is sufficient to show the convergence of $\mathcal{G}(q)$, $\langle\hat{X}^2(q)\rangle^{-1}$ and $\langle\hat{P}^2(q)\rangle$ that occur in the expression for LHA [Eq. 37].

The expression for the error estimate associated with LHA [Eq. 16] is derived in Appendix. C. The expression for $\Delta(q, \eta)$ and $\mathcal{E}(q)$, required during the error estimation, are given as [Appendix. C 1],

$$\Delta(q, \eta) = \max \left\{ \left| \frac{V_1(q)}{V_2(q)} \left(\frac{W(q)}{\langle\hat{X}^2(q)\rangle} - 1 \right) \right|, |\eta| \right\} \quad (50)$$

$$\mathcal{E}(q) = \sqrt{\langle\hat{X}^2(q)\rangle - \frac{1}{V_2(q)\beta}} \left(\sqrt{\frac{1}{V_2(q)\beta\langle\hat{X}^2(q)\rangle}} + 1 \right) \quad (51)$$

where,

$$W(q) = \frac{1}{m\beta} \sum_{n=-\infty}^{+\infty} \frac{(-1)^n}{\mathcal{A}_n(q)} \quad (52)$$

Finally, LHA in USC, high temperature and infinite cutoff limit is studied in Appendix. D.

B. EXPRESSION FOR LHA

1. Harmonic oscillator partition function

In this section, we are going to derive the expression for the HO partition function, \tilde{Z} [Eq. 43] for a generic HO potential given as,

$$V_{HO}(q) = \frac{1}{2}m\omega^2q^2 \quad (53)$$

Let us write any path $q(\tau)$ starting and ending at $q + \eta$ and $q - \eta$, respectively, in terms of the classical path for HO and deviation over it,

$$q(\tau) = q_{\text{cl}}(\tau) + \delta(\tau) \quad (54)$$

where $\delta(0) = 0 = \delta(\beta)$. Then, since the classical path is a local extremum, the action given in Eq. 3 becomes [62],

$$S_{HO}[q(\tau)] = S_{HO}[q_{\text{cl}}(\tau)] + S_{HO}[\delta(\tau)] \quad (55)$$

$$= S_{HO}[q_{\text{cl}}(\tau)] + \int_0^\beta d\tau \left(\frac{1}{2} m \dot{\delta}(\tau)^2 + V_{HO}(\delta(\tau)) \right) + \frac{1}{4} \int_0^\beta d\tau \int_0^\beta d\tau' K(\tau - \tau') (\delta(\tau) - \delta(\tau'))^2 \quad (56)$$

where $S_{HO}[q_{\text{cl}}(\tau)]$ is the action for the corresponding classical path $q_{\text{cl}}(\tau)$ for the HO, given by [46],

$$S_{HO}[q_{\text{cl}}(\tau)] = \frac{q^2}{2 \langle \hat{q}^2 \rangle} + 2 \langle \hat{p}^2 \rangle \eta^2 \quad (57)$$

Then, in Eq. 3, we have,

$$\rho_{HO}(q, \eta) = \tilde{Z}^{-1} e^{-S_{HO}[q_{\text{cl}}(\tau)]} \mathcal{I} \quad (58)$$

where, analogous to Eq. 44, we have,

$$\mathcal{I} = \int_0^0 \mathcal{D}\delta(\tau) e^{-S_{HO}[\delta(\tau)]} \quad (59)$$

Then, using the expression for $\rho_{HO}(q, \eta)$ from Eq. 47 and using Eq. 58 and Eq. 57, we can obtain an expression for \tilde{Z} as,

$$\tilde{Z} = \mathcal{I} \sqrt{2\pi \langle \hat{X}^2 \rangle} \quad (60)$$

2. The path integral for the quantum deviation about the classical path

In this section, we are going to derive the expression for $\mathcal{I}(q)$ [Eq. 44] and consequently $\mathcal{G}(q)$ [Eq. 46] and also derive the criteria for the convergence of these quantities. Let us do a Fourier series decomposition of $\delta(\tau)$ [Eq. 54] as,

$$\delta(\tau) \equiv \frac{1}{\beta} \sum_{n=-\infty}^{\infty} b_n e^{i\nu_n \tau} \quad (61)$$

1. Action in terms of fourier components

The main result of this subsection, given in Eq. 74, is to express $S_{HO}[\delta(\tau)]$ [Eq. 56] in terms of the Fourier components b_n of $\delta(\tau)$ [Eq. 61]. What follows is some routine but tedious math and one can skip directly to Eq. 74.

Given Eq. 61, the kinetic part of the action [Eq. 56] can be evaluated using,

$$\int_0^\beta d\tau \dot{\delta}(\tau)^2 = \frac{1}{\beta^2} \int_0^\beta d\tau \left(\frac{d}{d\tau} \sum_{n=-\infty}^{\infty} b_n e^{i\nu_n \tau} \right)^2 = \frac{1}{\beta} \sum_n \nu_n^2 |b_n|^2 \quad (62)$$

Here, we have used the fact that $b_{-n} = b_n^*$. The potential part of Eq. 56 can be evaluated as,

$$\int_0^\beta \delta(\tau)^2 = \frac{1}{\beta^2} \left(\sum_{n=-\infty}^{\infty} b_n e^{i\nu_n \tau} \right)^2 = \frac{1}{\beta} \sum_n |b_n|^2 \quad (63)$$

In order to evaluate the dissipative term, let us first expand the following expression,

$$\begin{aligned} (\delta(\tau) - \delta(\tau'))^2 &= \frac{1}{\beta^2} \left(\sum_n b_n e^{i\nu_n \tau} - \sum_m b_m e^{i\nu_m \tau'} \right)^2 \\ &= \frac{1}{\beta^2} \sum_p \sum_q b_p b_q e^{i(\nu_p + \nu_q)\tau} + \sum_p \sum_q b_p b_q e^{i(\nu_p + \nu_q)\tau'} - 2 \sum_p \sum_q b_p b_q e^{i(\nu_p \tau + \nu_q \tau')} \end{aligned} \quad (64)$$

Furthermore, let us first Fourier expand the influence functional as,

$$K(\tau - \tau') = \frac{m}{\beta} \sum_k \xi_k e^{i\nu_k(\tau - \tau')} \quad (65)$$

where we have [46],

$$\xi_n = \frac{1}{m} \int_0^\infty d\omega J(\omega) \frac{2\omega}{\nu_n^2 + \omega^2} \quad (66)$$

The dissipative term can then be evaluated as,

$$\int_0^\beta d\tau \int_0^\beta d\tau' K(\tau - \tau') (\delta(\tau) - \delta(\tau'))^2 = \frac{1}{\beta^2} \int_0^\beta d\tau \int_0^\beta d\tau' \frac{m}{\beta} \sum_k \xi_k e^{i\nu_k(\tau - \tau')} \left(\sum_n b_n e^{i\nu_n \tau} - \sum_m b_m e^{i\nu_m \tau'} \right)^2 \quad (67)$$

$$= \frac{m}{\beta^3} \int_0^\beta d\tau \int_0^\beta d\tau' \sum_k \xi_k e^{i\nu_k(\tau - \tau')} \left(\sum_p \sum_q \left(b_p b_q e^{i(\nu_p + \nu_q)\tau} + b_p b_q e^{i(\nu_p + \nu_q)\tau'} - 2b_p b_q e^{i(\nu_p \tau + \nu_q \tau')} \right) \right) \quad (68)$$

$$= \frac{m}{\beta^3} \left(\beta \int_0^\beta d\tau \sum_{p,q} 2\xi_0 b_p b_q e^{i(\nu_p + \nu_q)\tau} - 2 \int_0^\beta d\tau \int_0^\beta d\tau' \sum_{p,q,k} \xi_k b_p b_q e^{i(\nu_p + \nu_k)\tau + i(\nu_q - \nu_k)\tau'} \right) \quad (69)$$

$$= \frac{m}{\beta} \left(\sum_p 2\xi_0 b_p b_{-p} - 2 \sum_{p,q,k} \delta(p+k)\delta(q-k)\xi_k b_p b_q \right) \quad (70)$$

$$= \frac{2m}{\beta} \sum_p (\xi_0 - \xi_p) |b_p|^2 \quad \text{sum over } p \text{ and } q \text{ then rename } k \rightarrow p \quad (71)$$

$$= \frac{2m}{\beta} \sum_p (\zeta_p) |b_p|^2 \quad (72)$$

where we used $\zeta_p = \xi_0 - \xi_p$ [Eq. 42], which can be derived from Eq. 66 as,

$$\xi_0 - \xi_n = \frac{1}{m} \int_0^\infty d\omega \frac{J(\omega)}{\omega} \left(\frac{2\nu_n^2}{(\nu_n^2 + \omega^2)} \right) = \zeta_n \quad \text{from Eq. 42} \quad (73)$$

Finally, using the simplified expressions for the kinetic [Eq. 62], potential [Eq. 63] and dissipative [Eq. 72] part of the action Eq. 56, we have,

$$S_{HO}[\delta(\tau)] = \sum_{n=-\infty}^{\infty} \frac{1}{2} \frac{m}{\beta} |b_n|^2 (\nu_n^2 + \omega^2 + \zeta_n) \quad (74)$$

2. Calculating the deviation integral

Let us define,

$$\alpha_n \equiv \frac{m}{\beta} (\omega^2 + \nu_n^2 + \zeta_n) \quad (75)$$

The factor $\frac{1}{\alpha_n}$ gives an effective cutoff for the value of $|b_n|^2$ for each value of n . For any n , if $|b_n|^2$ crosses this cutoff, then the influence of the corresponding path will decay off rapidly. Let us move to the Cartesian coordinates, defining x_n and y_n as the real and imaginary parts of the complex number b_n (i.e., $x_n \equiv \Re(b_n)$ and $y_n \equiv \Im(b_n)$). Since $\delta(0) = 0$, the Fourier component of any function of this type must satisfy,

$$\sum_{n=-\infty}^{\infty} x_n = 0 \quad (76)$$

$$\implies x_0 = -2 \sum_{n=1}^{\infty} x_n \quad (77)$$

Hence, x_0 is not an independent parameter in the path integral. Similarly, since $x_{-n} = x_n$ and $y_{-n} = -y_n$, hence the only independent variables are those corresponding to $n \geq 1$. The path integral \mathcal{I} [Eq. 44] then becomes,

$$\mathcal{I} = J \left(\prod_{n=1}^{\infty} \int_{-\infty}^{\infty} dy_n \int_{-\infty}^{\infty} dx_n \right) \exp \left\{ -\frac{1}{2} \alpha_0 \left(2 \sum_{n=1}^{\infty} x_n \right)^2 - 2 \sum_{n=1}^{\infty} \frac{1}{2} \alpha_n (x_n^2 + y_n^2) \right\} \quad (78)$$

Here, J is the Jacobian coming from the linear transformation given in Eq. 61. We will now analytically evaluate this integral. But we should first note that this integral will diverge if for $n \geq 1$, $\alpha_n \leq 0$, which would break down LHA.

Before proceeding, note that we have $\alpha_{|n+1|} > \alpha_{|n|}$. This is true because $\nu_{|n+1|} > \nu_{|n|}$ follows from definition and immediately gives $\zeta_{|n+1|} > \zeta_{|n|}$ since $x/(a+x)$ monotonically increases for positive x and a . Hence, as a necessary condition for Eq. 78 to be convergent, we just need to impose that $\alpha_1 > 0$. We will hence restrict ourselves to this constraint. (As a side remark, note that this assumption automatically ensures the convergence of $\langle \hat{P}^2(q) \rangle$ [Eq. 39].) But it is still unclear whether $\alpha_0 \leq 0$ will lead to divergence in Eq. 78 or not. In this section, we will see that \mathcal{I} can be convergent even if $\alpha_0 \leq 0$.

After doing the y_n integral in Eq. 78, we get,

$$\mathcal{I} = J \left(\prod_{m=1}^{\infty} \sqrt{\frac{\pi}{\alpha_m}} \right) \left(\prod_{n=1}^{\infty} \int_{-\infty}^{\infty} dx_n \right) \exp \left\{ - \left(2\alpha_0 \left[\sum_{n=1}^{\infty} x_n \right]^2 + \sum_{n=1}^{\infty} \alpha_n x_n^2 \right) \right\} \quad (79)$$

Let us define the negative of the exponent above as,

$$\mathcal{F} \equiv \left(2\alpha_0 \left[\sum_{n=1}^{\infty} x_n \right]^2 + \sum_{n=1}^{\infty} \alpha_n x_n^2 \right) \quad (80)$$

If $\min_{x_n} \mathcal{F} > 0$, then \mathcal{I} will converge. We can think of \mathcal{F} as a diagonal component of a matrix M , i.e. $\mathcal{F} \equiv \langle v | M | v \rangle$ where, $\langle v | = \langle x_1, x_2, x_3, \dots |$ and $M = D + 2\alpha_0 J$ where, for $i, j \geq 1$, $J_{ij} = 1$ and $D_{ij} = \delta_{ij} \alpha_i$. Let λ_n be the eigenvalues of matrix M . Then we have,

$$\mathcal{I} = J \left(\prod_{n=1}^{\infty} \frac{\pi}{\sqrt{\alpha_n \lambda_n}} \right) \quad (81)$$

Before proceeding, let us first simplify an expression we will need immediately. From the definition of $\langle \hat{q}^2 \rangle$ [Eq. 38] and α_n [Eq. 75], we have,

$$\langle \hat{q}^2 \rangle = \frac{1}{\beta^2} \sum_{n=-\infty}^{\infty} \frac{1}{\alpha_n} \quad (82)$$

$$\implies 2 \sum_{n=1}^{\infty} \frac{1}{\alpha_n} = \beta^2 \langle \hat{q}^2 \rangle - \frac{1}{\alpha_0} \quad (83)$$

Proceeding with the derivation of \mathcal{I} again, we next need to calculate the value of the product $\prod_{n=1}^{\infty} \lambda_n$. We note that this is just given by the determinant of the matrix M , i.e.,

$$\prod_{n=1}^{\infty} \lambda_n = |M| \quad (84)$$

$$= \left(\prod_{n=1}^{\infty} \alpha_n \right) + 2\alpha_0 \left(\prod_{n=1}^{\infty} \alpha_n \right) \left(\sum_{m=1}^{\infty} \frac{1}{\alpha_m} \right) \quad (85)$$

$$= \left(\prod_{n=1}^{\infty} \alpha_n \right) \left(1 + \alpha_0 \left(\beta^2 \langle \hat{q}^2 \rangle - \frac{1}{\alpha_0} \right) \right) \quad \text{from Eq. 83} \quad (86)$$

$$= \alpha_0 \beta^2 \langle \hat{q}^2 \rangle \prod_{n=1}^{\infty} \alpha_n \quad (87)$$

We hence have,

$$\mathcal{I} = J \left(\frac{1}{\sqrt{\alpha_0 \beta^2 \langle \hat{q}^2 \rangle}} \prod_{n=1}^{\infty} \frac{\pi}{\alpha_n} \right) \quad (88)$$

This infinite product will give an infinitesimally small result because α_n scales as n^2 . But to get a reasonable result for LHA, we can proceed as follows. In the expression for LHA [Eq. 36], we effectively have a factor of, $\frac{\mathcal{I}(q)}{Z_R}$. Let us transform it as,

$$\frac{\mathcal{I}(q)}{Z_R} \equiv \frac{\mathcal{G}(q)}{Z} \quad (89)$$

where we define Z as,

$$Z = Z_R \left(\frac{1}{J} \prod_{n=1}^{\infty} \frac{\frac{m}{\beta} (\nu_n^2 + \zeta_n)}{\pi} \right) \quad (90)$$

We hence have, for $\mathcal{G}(q)$,

$$\mathcal{G} = \frac{Z}{Z_R} \mathcal{I} = \left(\frac{1}{J} \prod_{n=1}^{\infty} \frac{\frac{m}{\beta} (\nu_n^2 + \zeta_n)}{\pi} \right) \mathcal{I} \quad (91)$$

$$= \frac{1}{\sqrt{\alpha_0 \beta^2 \langle \hat{q}^2 \rangle}} \prod_{n=1}^{\infty} \frac{\alpha_n - \frac{m\omega^2}{\beta}}{\alpha_n} \quad (92)$$

This quantity can be shown to converge. On the other hand, Z serves as an overall normalization factor for LHA since, as we remarked in Appendix. A, it depends only upon $k_B T$, Ω and γ , but not on ω , and is hence independent of q . Note that the Jacobian J , coming from the linear transformation given in Eq. 61, is also ω independent.

Now, we are going to investigate the condition for Eq. 92 to converge. Since we have assumed $\alpha_{n \geq 1} > 0$, we note that for Eq. 92 to be real, we need,

$$\alpha_0 \langle \hat{q}^2 \rangle > 0 \quad (93)$$

$$\implies \alpha_0 \left(\frac{1}{\alpha_0} + 2 \sum_{n=1}^{\infty} \frac{1}{\alpha_n} \right) > 0 \quad \text{from Eq. 83} \quad (94)$$

If α_0 is also positive, then Eq. 94 is automatically satisfied. If $\alpha_0 < 0$, then we are interested in the highest value of α_0 such that we have,

$$\left(\frac{1}{\alpha_0} + 2 \sum_{n=1}^{\infty} \frac{1}{\alpha_n} \right) = 0 \quad (95)$$

$$\implies \sum_{n=1}^{\infty} \frac{\alpha_0}{\alpha_n} = -\frac{1}{2} \quad (96)$$

$$\implies \sum_{n=1}^{\infty} \frac{m\omega^2}{m\omega^2 + m\nu_n + m\zeta_n} = -\frac{1}{2} \quad (97)$$

Here, we used the definition of α_n [Eq. 75]. Redefining $m\omega^2 = -x$ and $m\nu_n^2 + m\zeta_n = y_n$, we get Eq. 13, where now we are interested in the smallest solution for x in the following equation,

$$\implies \sum_{n=1}^{\infty} \frac{x}{y_n - x} = \frac{1}{2} \quad (98)$$

The smallest solution for x gives us the value of V_P , defined in Sec. II, such that LHA will give convergent results for $V_2(q) > -V_P$.

Note that, from Eq. 93, for $\alpha_0 < 0$, we are equivalently interested in the highest negative value of ω^2 such that $\langle \hat{q}^2 \rangle = 0$. Hence, for the value of ω^2 higher than this, convergence of $\langle \hat{X}^2(q) \rangle^{-1}$ [Eq. 38] is also guaranteed, as required by LHA [Eq. 37] to be well defined. Also, since some spectral densities admit closed form expression for $\langle \hat{q}^2 \rangle$, this condition can easily be checked for in these cases.

In summary, we can say that LHA gives convergent results if,

- $\alpha_0 > 0$,
- $\alpha_0 < 0$ and $\alpha_1 > 0$, and Eq. 94 is true. The value of V_P is given as the smallest solution for x in Eq. 98.

C. ERROR ESTIMATION

In this section, we are going to derive the expression for the estimation of the error associated with LHA [Eq. 16]. We start with Eq. 3. Parameterising the path variable as $q(\tau) = q + \delta(\tau)$, where $q(\tau)$ starts and ends at points $q + \eta$ and $q - \eta$, respectively, we can write,

$$V(q + \delta) = V(q) + V_1(q)\delta + \frac{1}{2!}V_2(q)\delta^2 + \frac{1}{3!}V_3(q)\delta^3 + O(\delta^4) \quad (99)$$

Let us write the full action in terms of the quadratic part and higher order terms in the potential, as,

$$S[q + \delta(\tau)] = S_q[q + \delta(\tau)] + \int_0^\beta d\tau \sum_{n=3} \frac{1}{n!} V_n(q)\delta(\tau)^n \quad (100)$$

Then, writing the exact state $\sigma(q, \eta)$ in terms of harmonic action $S_q[q + \delta(\tau)]$ and higher order corrections over it, we get,

$$\sigma(q, \eta) = Z'^{-1} \left\{ \int_{-\eta}^{\eta} \mathcal{D}\delta(\tau) \exp \left(- \int_0^\beta d\tau \sum_{n=3} \frac{1}{n!} V_n(q)\delta(\tau)^n \right) e^{-S_q[q+\delta(\tau)]} \right\} \quad (101)$$

Here, Z' is the normalization factor defined as,

$$Z' = \int_{-\infty}^{\infty} dq \left\{ \int_0^0 \mathcal{D}\delta(\tau) \exp \left(- \int_0^\beta d\tau \sum_{n=3} \frac{1}{n!} V_n(q)\delta(\tau)^n \right) e^{-S_q[q+\delta(\tau)]} \right\} \quad (102)$$

Let us approximate Eq. 101 as,

$$\sigma(q, \eta) \approx \rho(q, \eta) - \sum_{n=3} \frac{V_n(q)}{n!} \left\{ \int_{-\eta}^{\eta} \mathcal{D}\delta(\tau) \left(\int_0^\beta d\tau \delta(\tau)^n \right) e^{-S_q[q+\delta(\tau)]} \right\} \quad (103)$$

$$\approx \rho(q, \eta) - \frac{V_3(q)}{3!} \left\{ \int_{-\eta}^{\eta} \mathcal{D}\delta(\tau) \left(\int_0^\beta d\tau \delta(\tau)^3 \right) e^{-S_q[q+\delta(\tau)]} \right\} \quad (104)$$

Here, $\rho(q, \eta)$ is the LHA state and in the last step, we have made a first order approximation. We now need to calculate the quantity,

$$I_3 = \int_{-\eta}^{\eta} \mathcal{D}\delta(\tau) \left(\int_0^\beta d\tau \delta(\tau)^3 \right) e^{-S_q[q+\delta(\tau)]} \quad (105)$$

Here, we are going to estimate this path integral using the following argument. Reparametrize $q + \delta(\tau) \rightarrow q_{\text{cl}}(\tau) + \delta(\tau)$. Then using $S_q[q + \delta(\tau)] \rightarrow S_q[q_{\text{cl}}(\tau) + \delta(\tau)] = S_q[q_{\text{cl}}(\tau)] + S_q[\delta(\tau)]$, we get,

$$I_3 = e^{-S_q[q_{\text{cl}}(\tau)]} \int_0^0 \mathcal{D}\delta(\tau) \left(\int_0^\beta d\tau (q_{\text{cl}}(\tau) - q + \delta(\tau))^3 \right) e^{-S_q[\delta(\tau)]} \quad (106)$$

Now, if n is an odd number, then we have $(-\delta(\tau))^n = -\delta(\tau)^n$. But since $S_q[-\delta(\tau)] = S_q[\delta(\tau)]$, when we take the full path integral, we get,

$$\int_0^0 \mathcal{D}\delta(\tau) \left(\int_0^\beta d\tau (q_{\text{cl}}(\tau) - q)^m \delta(\tau)^n \right) e^{-S_q[\delta(\tau)]} = 0 \quad \text{for odd } n \quad (107)$$

$$\implies I_3 = e^{-S_q[q_{\text{cl}}(\tau)]} \int_0^0 \mathcal{D}\delta(\tau) \left(\int_0^\beta d\tau ((q_{\text{cl}}(\tau) - q)^3 + 3(q_{\text{cl}}(\tau) - q)\delta(\tau)^2) \right) e^{-S_q[\delta(\tau)]} \quad (108)$$

Now, we are going to replace $q_{\text{cl}}(\tau) - q$ with its maximum value, given by $\Delta(q, \eta)$, and $\delta(\tau)$ with its typical value, given by $\mathcal{E}(q)$, to obtain,

$$I_3 \approx \beta (\Delta(q, \eta)^3 + 3\mathcal{E}(q)^2 \Delta(q, \eta)) \int_{-\eta}^{\eta} \mathcal{D}\delta(\tau) e^{-S_a[q+\delta(\tau)]} \quad (109)$$

We will estimate $\Delta(q, \eta)$ and $\mathcal{E}(q)$ in [Sec. C 1](#).

Let's define a quantity, $\mathcal{T}(q, \eta)$, as a measure of the relative error corresponding to the matrix element $\rho(q, \eta)$ as,

$$\mathcal{T}(q, \eta) \equiv -\beta \frac{V_3}{3!} (\Delta(q, \eta)^3 + 3\mathcal{E}(q)^2 \Delta(q, \eta)) \quad (110)$$

Also, for convenience, let us define,

$$\epsilon_T \equiv \int dq \rho(q) |\mathcal{T}(q)| \quad (111)$$

$$= \langle |\mathcal{T}(q)| \rangle \quad (112)$$

Then, [Eq. 101](#) becomes,

$$\sigma(q, \eta) \approx \frac{\rho(q, \eta) \pm \rho(q, \eta) |\mathcal{T}(q, \eta)|}{Z'} \quad (113)$$

$$= \frac{\rho(q, \eta) \pm \rho(q, \eta) |\mathcal{T}(q, \eta)|}{1 \pm \epsilon_T} \quad (114)$$

$$\approx \rho(q, \eta) \pm \epsilon(q, \eta) \rho(q, \eta) \quad (115)$$

where,

$$\epsilon(q, \eta) = |\mathcal{T}(q, \eta)| + \epsilon_T \quad (116)$$

gives a measure of the total relative error for the matrix element $\rho(q, \eta)$. To get an expression for the relative error associated with an observable \hat{O} , we define,

$$\epsilon_{\hat{O}} = \frac{1}{\langle \hat{O} \rangle} \int dq \int d\eta \hat{O}(q, \eta) \epsilon(q, \eta) |\rho(q, \eta)| \quad (117)$$

1. Length Scale estimation

In the following subsections, we will estimate $\Delta(q, \eta)$ and $\mathcal{E}(q)$. Let $q_{\text{cl}}(\tau)$ be the classical path for an HO, starting and ending at points $q + \eta$ and $q - \eta$, respectively, given by,

$$q_{\text{cl}}(\tau) = \frac{1}{\beta} \sum_{n=-\infty}^{\infty} a_n e^{i\nu_n \tau} \quad (118)$$

Then, a_n is given as [\[46\]](#),

$$a_n = \left\{ \left(\frac{i\nu_n}{\omega^2 + \nu_n^2 + \zeta_n} \right) 2\eta + \frac{1}{\omega^2 + \nu_n^2 + \zeta_n} \frac{q}{m \langle \hat{q}^2 \rangle} \right\} \quad (119)$$

We conjecture that for $\eta = 0$, $|q_{\text{cl}}(\tau) - q|$ will have its global maxima at $\tau = \beta/2$. This intuition rests on the fact that in the general path integral equation [\[Eq. 3\]](#), although the potential term will push the extremum classical path towards the potential minima, the kinetic and dissipative terms will help remove any oscillations from it. Hence, the curve will have a single extrema, and since for $\eta = 0$, the classical path can be seen to be made up of only cosine Fourier components and hence is symmetric about $\tau = \beta/2$, therefore this extrema will be at $\tau = \beta/2$. We have also verified this numerically. When $\eta \neq 0$, we note that although the classical path still does not have any oscillations, $\tau = \beta/2$ does not give the extremum point anymore, but we assume that the maximum among $|q_{\text{cl}}(\beta/2) - q|$ and $|\eta|$ still gives a rough estimate for the maximum deviation of the classical path from the constant path $q'(\tau) = q$.

We will hence use the quantity $q_{\text{cl}}(\beta/2) - q$ to estimate $\Delta(q, \eta)$. We simplify this expression as,

$$q_{\text{cl}}(\beta/2) - q = -q + \frac{1}{\beta} \sum_{n=-\infty}^{\infty} (-1)^n a_n \quad (120)$$

$$= q \left(\frac{1}{m\beta \langle \hat{q}^2 \rangle} \sum_{n=-\infty}^{\infty} \frac{(-1)^n}{\nu_n^2 + \omega^2 + \zeta_n} - 1 \right) \quad (121)$$

Hence, the estimate for the maximum deviation of the classical path is then given by,

$$\Delta_{HO}(q, \eta) = \max \left\{ \left| q \left(-1 + \frac{1}{m\beta \langle \hat{q}^2 \rangle} \sum_{n=-\infty}^{\infty} \frac{(-1)^n}{\nu_n^2 + \omega^2 + \zeta_n} \right) \right|, |\eta| \right\} \quad (122)$$

Relating $q \equiv V_1(q)/V_2(q)$ [Eq. 11], we directly recover the expression for the maximum deviation of the classical path claimed earlier [Eq. 50].

Next, in order to estimate $\mathcal{E}(q)$, rename $r_n \equiv |b_n|$ [Eq. 74] and write the path integral for \mathcal{I} [Eq. 78] in polar coordinate as,

$$\mathcal{I} = J \left(\prod_{n=1}^{\infty} \int_0^{\infty} dr_n \int_0^{2\pi} r_n d\theta_n \right) e^{-(\frac{1}{2}\alpha_0 b_0^2 + 2 \sum_{n=1}^{\infty} \frac{1}{2}\alpha_n r_n^2)} \quad (123)$$

Note that θ_n dependence in the integrand is in b_0 and comes through the following constraint [Eq. 76],

$$b_0 = -2 \sum_{n=1}^{\infty} \Re(b_n) \quad (124)$$

We are now in the position to immediately do all the $d\theta_n$ integrals in the Eq. 123. For this, we note that for a fixed value of b_n 's, where $n = 0, 1, 2, \dots$, the $d\theta_n$ integrals in Eq. 123 give us a measure of all the configurations that satisfy the constraint in Eq. 124.

Now consider a 2D random walk starting from origin, where the n th step size for the walk is given by the function $\mathcal{S}(n) = 2|b_n| = 2r_n$. Then after $N \rightarrow \infty$ steps, the probability distribution $P(x)$ for this walker to have the x-axis position value of $-b_0$ gives a measure that is equivalent to doing all the $d\theta_n$ integrals in Eq. 123. Note that there is a factor of 2 in the definition for $\mathcal{S}(n)$ because of the corresponding factor of 2 in Eq. 124.

This probability distribution is given as [63],

$$P(x) = \frac{1}{\sigma} \sqrt{\frac{1}{2\pi}} e^{-\frac{x^2}{2\sigma^2}} \quad (125)$$

where, the variance σ^2 is given by,

$$\sigma^2 = \frac{1}{2} \sum_{n=1}^{\infty} (\mathcal{S}(n))^2 \quad (126)$$

$$= 2 \sum_{n=1}^{\infty} r_n^2 \quad (127)$$

Note that the Gaussian probability distribution for the random walk is true only if a few sets of steps, $\mathcal{S}(n)$, do not dominate over the others in size. If this is not the case, the actual distribution is more complicated (although it is still a decaying function with some width), and is given in terms of Bessel functions [63]. Here, for simplicity, we assume Gaussian probability distribution.

We hence replace all the $d\theta_n$ integrals with a single integral over the variable b_0 , and Eq. 123 becomes,

$$\mathcal{I} = J \left(\prod_{n=1}^{\infty} \int_0^{\infty} r_n dr_n \right) \int_{-R}^R db_0 \frac{1}{\sigma} \sqrt{\frac{1}{2\pi}} e^{-(\frac{1}{2}(\alpha_0 + \frac{1}{\sigma^2})b_0^2 + 2 \sum_{n=1}^{\infty} \frac{1}{2}\alpha_n r_n^2)} \quad (128)$$

where $R = 2 \sum_{n=1}^{\infty} r_n$ is put here to ensure that Eq. 124 is not violated.

Note that this equation gives a typical length-scale for the value for r_n and b_0 as following,

$$r_n^2 = |b_n|^2 \approx \frac{1}{\alpha_n} \quad (129)$$

$$\implies \sigma^2 \approx 2 \sum_{n=1}^{\infty} \frac{1}{\alpha_n} \quad \text{from Eq. 127} \quad (130)$$

$$\implies b_0^2 \approx \frac{1}{\alpha_0 + \frac{1}{2 \sum_{n=1}^{\infty} \frac{1}{\alpha_n}}} \quad (131)$$

Using the typical value of $|b_n|$ from here, we can go back in the position space representation of $\delta(\tau)$ [Eq. 61] that corresponds to the paths that have important contribution to \mathcal{I} , as,

$$\delta(\tau) = \frac{1}{\beta} \left(\frac{1}{\sqrt{\alpha_0 + \frac{1}{2 \sum_{n=1}^{\infty} \frac{1}{\alpha_n}}}} + \sum_{n \neq 0} \frac{1}{\sqrt{\alpha_n}} e^{i\theta_n} e^{i\nu_n \tau} \right) \quad (132)$$

where, $\theta_{-n} = -\theta_n$ are random phases with the condition, coming from Eq. 124, that $\delta(\tau = 0) = 0$.

We are interested in the typical deviation of $\delta(\tau)$. To simplify the problem, we now relax the condition $\delta(\tau = 0) = 0$ so that θ_n become truly random and this again reduces to the random walk problem with fixed step size [63]. To be precise, the mathematical problem we are now dealing with is- given a Fourier series with fixed coefficients but random phases ϕ_n ,

$$h(x) = c_0 + \sum_{n=1}^{\infty} c_n \sin(2\pi n x + \phi_n) \quad (133)$$

What is the probability density, $P(y)$, that $h(x) = y$ for any given value of x ?

Using similar random walk arguments as used before, $P(y)$ can be shown to be approximately given by,

$$P(y) = \frac{1}{\sigma} \sqrt{\frac{1}{2\pi}} e^{-\frac{(y-c_0)^2}{2\sigma^2}} \quad (134)$$

where σ is given by,

$$\sigma = \sqrt{\frac{1}{2} \sum_{n=1}^{\infty} c_n^2} \quad (135)$$

An estimate for $\mathcal{E}_{HO}(q)$ can now be given by,

$$\mathcal{E}_{HO}(q) = c_0 + \sigma \quad (136)$$

For our case, from Eq. 132, we have,

$$c_0 = \frac{1}{\beta} \frac{1}{\sqrt{\alpha_0 + \frac{1}{2 \sum_{n=1}^{\infty} \frac{1}{\alpha_n}}}} \quad (137)$$

$$c_{n \geq 1} = \frac{1}{\beta} \frac{2}{\sqrt{\alpha_n}} \quad (138)$$

Let us first simplify the following expression,

$$\frac{1}{\alpha_0 + \frac{1}{2 \sum_{n=1}^{\infty} \frac{1}{\alpha_n}}} = \frac{1}{\alpha_0 + \frac{1}{\beta^2 \langle \hat{q}^2 \rangle - \frac{1}{\alpha_0}}} \quad \text{from Eq. 83} \quad (139)$$

$$= \frac{\beta^2 \langle \hat{q}^2 \rangle - \frac{1}{\alpha_0}}{\alpha_0 \beta^2 \langle \hat{q}^2 \rangle} \quad (140)$$

Hence, from Eq. 135, Eq. 136, Eq. 137 and Eq. 138, we have,

$$\mathcal{E}_{HO}(q) = \frac{1}{\beta} \left(\sqrt{\frac{\beta^2 \langle \hat{q}^2 \rangle - \frac{1}{\alpha_0}}{\alpha_0 \beta^2 \langle \hat{q}^2 \rangle}} + \sqrt{\beta^2 \langle \hat{q}^2 \rangle - \frac{1}{\alpha_0}} \right) \quad \text{from Eq. 83} \quad (141)$$

$$= \sqrt{\langle \hat{q}^2 \rangle - \frac{1}{\beta^2 \alpha_0}} \left(\sqrt{\frac{1}{\alpha_0 \beta^2 \langle \hat{q}^2 \rangle}} + 1 \right) \quad (142)$$

$$= \sqrt{\langle \hat{q}^2 \rangle - \frac{1}{m\omega^2 \beta}} \left(\sqrt{\frac{1}{m\omega^2 \beta \langle \hat{q}^2 \rangle}} + 1 \right) \quad (143)$$

where we have used $\alpha_0 = \frac{m\omega^2}{\beta}$ from Eq. 75. This recovers the expression for $\mathcal{E}(q)$ [Eq. 51], the typical quantum deviation of all the paths about $q_{cl}(\tau)$ that have significant contribution to the action.

D. SPECIAL CASES

1. Ultra strong coupling limit

In the ultra strong coupling limit, i.e., $\lim_{J(\omega) \rightarrow \infty}$, first note that, from the definition of ζ_n [Eq. 42], we have,

$$\lim_{J(\omega) \rightarrow \infty} \zeta_{n \neq 0} = \infty \quad (144)$$

From the definition of $\langle \hat{X}^2(q) \rangle$ [Eq. 38], we have,

$$\lim_{J(\omega) \rightarrow \infty} \langle \hat{X}^2(q) \rangle = \lim_{J(\omega) \rightarrow \infty} \frac{1}{m\beta} \sum_{n=-\infty}^{+\infty} \frac{1}{\frac{V_2(q)}{m} + \nu_n^2 + \zeta_n} \quad (145)$$

$$= \frac{1}{\beta V_2(q)} \quad (146)$$

Similarly, from definition of $\langle \hat{P}^2(q) \rangle$ [Eq. 39], we have,

$$\lim_{J(\omega) \rightarrow \infty} \langle \hat{P}^2(q) \rangle = \frac{m}{\beta} + 2 \sum_{n=1}^{+\infty} \lim_{\zeta_n \rightarrow \infty} \frac{\frac{V_2(q)}{m} + \zeta_n}{\frac{V_2(q)}{m} + \nu_n^2 + \zeta_n} \quad (147)$$

$$= \frac{m}{\beta} + 2 \sum_{n=1}^{+\infty} 1 \quad (148)$$

$$= \infty \quad (149)$$

Finally, from definition of $\mathcal{G}(q)$ [Eq. 46], we have,

$$\lim_{J(\omega) \rightarrow \infty} \mathcal{G}(q) = \lim_{J(\omega) \rightarrow \infty} \frac{1}{\sqrt{V_2(q)\beta \langle \hat{X}^2(q) \rangle}} \prod_{n=1}^{\infty} \frac{\nu_n^2 + \zeta_n}{\mathcal{A}_n(q)} \quad (150)$$

$$= \lim_{J(\omega) \rightarrow \infty} \frac{1}{\sqrt{V_2(q)\beta \frac{1}{\beta V_2(q)}}} \prod_{n=1}^{\infty} 1 \quad (151)$$

$$= 1 \quad (152)$$

Hence expression for USC-LHA [Eq. 37] becomes,

$$\lim_{J(\omega) \rightarrow \infty} \rho(q, \eta) = \delta(\eta) Z^{-1} \exp \left(-\frac{(V_1(q)/V_2(q))^2}{2 \langle \hat{X}^2(q) \rangle} - \beta \left(V(q) - \frac{V_1(q)^2}{2V_2(q)} \right) \right) \quad (153)$$

$$\implies \lim_{J(\omega) \rightarrow \infty} \rho(q) = Z^{-1} \exp(-\beta V(q)) \exp \left(-\frac{\beta V_1(q)^2}{2V_2(q)} + \frac{\beta V_1(q)^2}{2V_2(q)} \right) \quad (154)$$

$$= Z^{-1} \exp(-\beta V(q)) \quad (155)$$

which is the CV version of the USC result [25]. To see this equivalence, note that the USC result is usually stated as,

$$\rho = Z_{USC}^{-1} \exp \left(-\beta \sum_n P_n H_s P_n \right) \quad (156)$$

where $P_n = |x_n\rangle \langle x_n|$ are projection operators on the non-degenerate eigenstates $|x_n\rangle$ of the system coupling operators X and Z_{USC} is a normalization factor.

We note that in the CV limit,

$$\sum_n P_n H_s P_n = \int dq \left(\frac{\langle q | \hat{P}^2 | q \rangle}{2m} + V(q) \right) |q\rangle \langle q| \quad (157)$$

Now, $\sum_q \langle q | \hat{P}^2 | q \rangle |q\rangle \langle q|$ is proportional to the identity operator, and hence will commute with the potential operator. Therefore, in the expression for the USC-MFGS, the contribution of the momentum operator can be absorbed in the trace and we recover Eq. 155 as the USC result.

Now, let us calculate $\Delta(q, \eta)$ in this limit. Let us first evaluate $W(q)$ [Eq. 52] that comes up in the definition of $\Delta(q, \eta)$ as,

$$\lim_{J(\omega) \rightarrow \infty} W(q) = \frac{1}{\beta V_2(q)} + \frac{1}{m\beta} \sum_{n=1}^{+\infty} \lim_{\zeta_n \rightarrow \infty} \frac{(-1)^n}{\frac{V_2(q)}{m} + \nu_n^2 + \zeta_n} \quad (158)$$

$$= \frac{1}{\beta V_2(q)} \quad (159)$$

Hence, from the definition of $\Delta(q, \eta)$ [Eq. 50], we have,

$$\lim_{J(\omega) \rightarrow \infty} \Delta(q, \eta) = \max \left\{ \left| \lim_{J(\omega) \rightarrow \infty} \frac{V_1(q_0)}{V_2(q_0)} \left(1 - \frac{W(q_0)}{\langle \hat{X}^2(q_0) \rangle} \right) \right|, |\eta| \right\} \quad (160)$$

$$= \max \left\{ \left| \frac{V_1(q_0)}{V_2(q_0)} \left(1 - \frac{\frac{1}{\beta V_2(q)}}{\frac{1}{\beta V_2(q)}} \right) \right|, |\eta| \right\} \quad (161)$$

$$= \max \{0, |\eta|\} \quad (162)$$

$$(163)$$

Similarly, let us calculate $\mathcal{E}(q)$ in this limit. From the definition of $\mathcal{E}(q)$ [Eq. 51], we have,

$$\lim_{J(\omega) \rightarrow \infty} \mathcal{E}(q) = \lim_{J(\omega) \rightarrow \infty} \sqrt{\langle \hat{X}^2(q) \rangle - \frac{1}{V_2(q)\beta}} \left(\sqrt{\frac{1}{V_2(q)\beta \langle \hat{X}^2(q) \rangle}} + 1 \right) \quad (164)$$

$$= \sqrt{\frac{1}{V_2(q)\beta} - \frac{1}{V_2(q)\beta}} \left(\sqrt{\frac{1}{V_2(q)\frac{1}{V_2(q)\beta}}} + 1 \right) \quad (165)$$

$$= 0 \quad (166)$$

Hence, we note that both $\Delta(q, \eta)$ and $\mathcal{E}(q)$ have expected behavior in the USC limit.

2. High temperature limit

To understand why LHA becomes accurate in the high temperature limit, consider an arbitrary path $q(\tau)$ starting and ending at the points $q + \eta$ and $q - \eta$, respectively. Now, for $a > 1$, let us rescale $\beta \rightarrow \beta/a$ such that we have $q(\tau) \rightarrow q_a(\tau) \equiv q(a\tau)$, where we have identified the paths $q(\tau)$ and $q_a(\tau)$ with each other through a one-to-one and onto map. Note that we have $q(0) = q + \eta = q_a(0)$ and $q(\beta) = q - \eta = q_a(\beta/a)$. Now, define the new action, $S_a[q_a(\tau)]$ as,

$$S_a[q_a(\tau)] = \int_0^{\beta/a} d\tau \left(\frac{1}{2} m \dot{q}_a(\tau)^2 + V(q_a(\tau)) \right) + \frac{1}{4} \int_0^{\beta/a} d\tau \int_0^{\beta/a} d\tau' K_a(\tau - \tau') (q_a(\tau) - q_a(\tau'))^2 \quad (167)$$

where,

$$K_a(\tau) = \int_0^\infty d\omega J(\omega) \frac{\cosh[\omega(\beta/2a - \tau)]}{\sinh[\omega\beta/2a]} \quad (168)$$

Then, we have,

$$\int_0^{\beta/a} \frac{d^2}{d\tau^2} q_a(\tau) d\tau = a^2 \int_0^{\beta/a} \frac{d^2}{d(a\tau)^2} q(a\tau) d\tau \quad (169)$$

$$= a \int_0^\beta \frac{d^2}{d\tau^2} q(\tau) d\tau \quad (170)$$

Similarly, we have,

$$\int_0^{\beta/a} V(q_a(\tau)) d\tau = \frac{1}{a} \int_0^\beta V(q(\tau)) d\tau \quad (171)$$

Before moving to the dissipative term, we write the hyperbolic factor coming in the correlation function [Eq. 168] in large a limit for $0 \leq \tau \leq \beta/a$ as,

$$\lim_{a \gg 1} \frac{\cosh[\omega(\beta/2a - \tau)]}{\sinh[\omega\beta/2a]} = \frac{2a}{\omega\beta} \quad (172)$$

For the dissipative term, T_D , in Eq. 167, we then have,

$$T_D = \lim_{a \gg 1} \int_0^{\beta/a} d\tau' \int_0^{\beta/a} d\tau K_a(\tau - \tau') (q_a(\tau) - q_a(\tau'))^2 \quad (173)$$

$$= \lim_{a \gg 1} \int_0^\infty d\omega J(\omega) \int_0^{\beta/a} d\tau' \int_0^{\beta/a} d\tau \frac{\cosh[\omega(\beta/2a - (\tau - \tau'))]}{\sinh[\omega\beta/2a]} (q(a\tau) - q(a\tau'))^2 \quad (174)$$

$$\approx \lim_{a \gg 1} \int_0^\infty d\omega J(\omega) \int_0^{\beta/a} d\tau' \int_0^{\beta/a} d\tau \frac{2a}{\omega\beta} (q(a\tau) - q(a\tau'))^2 \quad (175)$$

$$\approx \lim_{a \gg 1} \frac{1}{a} \int_0^\infty d\omega J(\omega) \int_0^\beta d\tau' \int_0^\beta d\tau \frac{2}{\omega\beta} (q(\tau) - q(\tau'))^2 \quad (176)$$

Hence, for large a , while the potential and dissipative terms scale as $1/a$, the kinetic term scales as a , dominating in high temperature limit and causing the paths with large variation to contribute less.

Analogous to the USC limit [Appendix. D 1], the high temperature limit gives us the following values for the relevant quantities,

$$\lim_{\beta \rightarrow 0} \langle \hat{X}^2(q) \rangle = \frac{1}{\beta V_2(q)} \quad (177)$$

$$\lim_{\beta \rightarrow 0} \langle \hat{P}^2(q) \rangle = \frac{m}{\beta} \quad (178)$$

$$\lim_{\beta \rightarrow 0} \mathcal{G}(q) = 1 \quad (179)$$

Hence the high temperature limit for the expression of LHA [Eq. 37] is given as,

$$\lim_{\beta \rightarrow 0} \rho(q, \eta) = \lim_{\beta \rightarrow 0} Z^{-1} \exp \left(-\frac{\beta V_2(q)}{2} \left(\frac{V_1(q)}{V_2(q)} \right)^2 - \frac{m}{2\beta} \eta^2 - \beta \left(V(q) - \frac{V_1(q)^2}{2V_2(q)} \right) \right) \quad (180)$$

$$\implies \lim_{\beta \rightarrow 0} \rho(q) = Z^{-1} \exp(-\beta V(q)) \quad (181)$$

We will now show that this high temperature MFGS is equivalent to the ones recently derived in literature [25, 43, 44]. Timofeev et al.[43] have shown that in the high temperature limit, at arbitrary coupling, the general Hamiltonian of mean force, H_{MF} , is given as,

$$H_{MF} = \sum_n \langle n | H_S | n \rangle + \sum_{n \neq m} \langle n | H_S | m \rangle \exp\{-\beta \Lambda (q_n - q_m)^2 / 6\} | n \rangle \langle m | \quad (182)$$

where $\Lambda \equiv \int_0^\infty d\omega J(\omega)/\omega$ and q_n are the eigenvalues of the system coupling operator \hat{q} . Note that Eq. 182 differs from the one obtained by the Timofeev et al. by a term of $-\Lambda\hat{q}^2$ because their definition of the free Hamiltonian includes the counterterm. For a CV system, Eq. 182 translates into,

$$H_{MF} = \left(\int dx V(x) |x\rangle \langle x| \right) + \left(\int \int dx dy \frac{\langle x | \hat{P}^2 | y \rangle}{2m} \exp \left\{ -\beta \Lambda \frac{(x-y)^2}{6} \right\} |y\rangle \langle x| \right) \quad (183)$$

Let us first set $\Lambda = 0$ for simplicity. Then, we have,

$$\Rightarrow \exp\{-\beta \hat{H}_{MF}\} \approx \exp\{-\beta V(x)\} \times \exp \left\{ -\beta \frac{\hat{P}^2}{2m} \right\} + O(\beta^2) \quad (184)$$

Let us focus on the second term,

$$\langle x | \exp(-\beta \hat{P}^2/2m) | y \rangle = \sqrt{\frac{m}{2\pi\beta}} \exp \left\{ -\frac{m}{2\beta} (x-y)^2 \right\} \quad (185)$$

$$\approx \delta(x-y) \quad \text{in high temperature limit} \quad (186)$$

We hence recover the high temperature MFGS result [Eq. 181]. Note that when $\Lambda \neq 0$, then the off-diagonal elements of H_{MF} [Eq. 183] get further suppressed and it can be formally shown that the exponential of the second term in Eq. 183 gets closer to $\delta(x-y)$ as compared with the $\Lambda = 0$ case, and hence Eq. 181 remains the high temperature MFGS.

We will now calculate $\Delta(q, \eta)$ [Eq. 50] and $\mathcal{E}(q)$ [Eq. 51] in the high temperature limit. For $\Delta(q, \eta)$, we first evaluate,

$$\lim_{\beta \rightarrow 0} \frac{V_1(q)}{V_2(q)} \left(1 - \frac{W(q)}{\langle \hat{X}^2(q) \rangle} \right) = \lim_{\beta \rightarrow 0} \frac{V_1(q)}{V_2(q)} \left(1 - \frac{\sum_{n=-\infty}^{+\infty} \frac{(-1)^n}{\frac{V_2(q)}{M} + \nu_n^2 + \zeta_n}}{\sum_{n=-\infty}^{+\infty} \frac{1}{\frac{V_2(q)}{M} + \nu_n^2 + \zeta_n}} \right) \quad (187)$$

$$= \lim_{\beta \rightarrow 0} \frac{V_1(q)}{V_2(q)} \left(1 - \frac{M}{\frac{V_2(q)}{M}} \right) \quad (188)$$

$$= 0 \quad (189)$$

We then have,

$$\lim_{\beta \rightarrow 0} \Delta(q, \eta) = |\eta| \quad (190)$$

Similarly, for $\mathcal{E}(q)$, we have,

$$\lim_{\beta \rightarrow 0} \mathcal{E} = \lim_{\beta \rightarrow 0} \sqrt{\langle \hat{q}^2 \rangle - \frac{1}{m\omega^2\beta}} \left(\sqrt{\frac{1}{m\omega^2\beta \langle \hat{q}^2 \rangle}} + 1 \right) \quad (191)$$

$$= 2 \lim_{\beta \rightarrow 0} \sqrt{\frac{2}{m\beta} \sum_{n=1}^{\infty} \frac{1}{\omega^2 + \nu_n^2 + \zeta_n}} \quad (192)$$

$$= 0 \quad (193)$$

Since these length scales become smaller as the temperature is increased, we infer that LHA becomes more accurate in the process.

3. High bath cutoff limit

Let Ω denote the bath cutoff frequency. Then in the limit $\Omega \rightarrow \infty$, we have,

$$\lim_{\Omega \rightarrow \infty} \int_0^\infty \frac{J(\omega)}{\omega} d\omega = \infty \quad (194)$$

From the definition of ζ_n [Eq. 42], we have,

$$\lim_{n \rightarrow \infty} \zeta_n = \frac{1}{m} \int_0^\infty \frac{J(\omega')}{\omega'} d\omega' \quad (195)$$

$$= \infty \quad (196)$$

$$\implies \lim_{n \rightarrow \infty} \frac{\omega^2 + \zeta_n}{\omega^2 + \nu_n^2 + \zeta_n} = 1 \quad (197)$$

$$\implies \lim_{n \rightarrow \infty} \sum_{n=1}^{\infty} \frac{\omega^2 + \zeta_n}{\omega^2 + \nu_n^2 + \zeta_n} = \infty \quad (198)$$

$$\implies \langle \hat{P}^2(q) \rangle = \infty \quad (199)$$

Here we have used the definition of $\langle \hat{P}^2(q) \rangle$ [Eq. 39]. Since $\langle \hat{P}^2(q) \rangle$ diverges, in this limit, LHA [Eq. 37] will not have coherence in the position basis, and therefore will be given by,

$$\rho(q, \eta) = \delta(\eta) Z^{-1} \mathcal{G}(q) \exp \left(-\frac{1}{2 \langle \hat{X}^2(q) \rangle} \left(\frac{V_1(q)}{V_2(q)} \right)^2 - \beta \left(V(q) - \frac{V_1(q)^2}{2V_2(q)} \right) \right) \quad (200)$$
